arXiv:1611.08967v1 [math.NA] 28 Nov 2016

A Stopping Criterion for The Multigrid Finite Element*

Zhiqiang Cai† Shuhao Cao‡ Rob Falgout§

Abstract

This paper introduces a reliable and efficient localized duality-type error estimator for total energy error of the multigrid finite element. The algebraic error is estimated by the extrapolated multigrid rate of convergence and the difference between two consecutive iterates. A stopping criteria is proposed to save the multigrid algorithm from over-solving. Implementation of the localized error estimation is illustrated using a minimally user-provided data structure such as the one in *hypre*.

1 Introduction

Consider the Dirichlet boundary value problem in a bounded polygonal/polyhedral domain $\Omega \subset \mathbb{R}^d$ $(d = 2, 3)$ for the diffusion-reaction equation as follows:

$$\begin{cases} -\nabla\cdot(A\nabla u) = f, & \text{in } \Omega, \\ u = g, & \text{on } \partial\Omega, \end{cases} \tag{1.1}$$

where the data $f \in L^2(\Omega)$.

In practice, the linear system from finite element approximation problem to (1.1) is solved using a multigrid iterative solver (either geometric V/W/F-cycles or AMG). Instead of having the exact solution $u_{\mathcal{T}}$ to the finite dimensional linear system at hand, $\bar{u}_{\mathcal{T}}$ is the current output from the solver. $\bar{u}_{\mathcal{T}} = u_{\mathcal{T}}^{(k)}$ if the k is the number of iterations. The following total energy error of $\bar{u}_{\mathcal{T}}$ to the solution u of the continuous weak problem (2.1) is to be measured (for the norm notations please refer to Section 2):

$$\underbrace{\|u - \bar{u}_{\mathcal{T}}\|_A^2}_{\text{total error}} = \underbrace{\|u_{\mathcal{T}} - \bar{u}_{\mathcal{T}}\|_A^2}_{\text{algebraic error}} + \underbrace{\|u - u_{\mathcal{T}}\|_A^2}_{\text{discretization error}}, \tag{1.2}$$

*This work performed under the auspices of the U.S. Department of Energy by Lawrence Livermore National Laboratory under Contract DE-AC52-07NA27344 (LLNL-JRNL-645325). This work was supported in part by the National Science Foundation under grants DMS-1320608, DMS-1418934, and DMS-1522707.

†Department of Mathematics, Purdue University, 150 N. University Street, West Lafayette, IN 47907-2067, zcai@math.purdue.edu.

‡Department of Mathematics, Pennsylvania State University, University Park, State College, PA 16802, scao@psu.edu.

§Center for Applied Scientific Computing, Lawrence Livermore National Laboratory, Livermore, CA 94551-0808, falgout2@llnl.gov.

where $\|\cdot\|_A$ is the energy norm associated with the problem (2.1) (please refer to Section 2 for details).

The goal of this paper is to propose a stopping criterion for the aforementioned iterative solver. Suppose after k iterations, the algebraic error $\left\|u_{\mathcal{T}} - u_{\mathcal{T}}^{(k)}\right\|_A$ has the same order of magnitude with the discretization error $\|u - u_{\mathcal{T}}\|_A$, and their ratio is a relatively small constant. Then by (1.2): the total error can be bounded by

$$\left\|u - u_{\mathcal{T}}^{(k)}\right\|_A \leq C \|u - u_{\mathcal{T}}\|_A . \tag{1.3}$$

Suppose the operator associated with the iterative solver has the contraction property, then performing another iteration of the solver reduces the algebraic error by an amount being the same order with the discretization error:

$$\left\|u_{\mathcal{T}} - u_{\mathcal{T}}^{(k+1)}\right\|_A \leq \left\|u_{\mathcal{T}} - u_{\mathcal{T}}^{(k)}\right\|_A \leq \left\|u - u_{\mathcal{T}}^{(k)}\right\|_A \leq C \|u - u_{\mathcal{T}}\|_A . \tag{1.4}$$

As a result, it is reasonable to stop. Because heuristically speaking, the current iterate $\bar{u}_{\mathcal{T}}^{(k)}$ is as close as $u_{\mathcal{T}}$, in terms of order, to the true solution u of the underlying PDE. To this end, a computable total error estimator estimating total energy error $\|u - \bar{u}_{\mathcal{T}}\|_A$ is constructed, as well as an algebraic error estimator estimating the algebraic error $\|u_{\mathcal{T}} - \bar{u}_{\mathcal{T}}\|_A$. And the stopping criterion of the iterative solver is based on comparing the magnitude of these two, provided that the estimators are representing their error counterparts reliably enough.

The first result concerning the total error in the adaptive finite element method (AFEM) is presented in the paper [6]. The same authors studied the idea further in [32, 30], leading to the Dual Weighted Residual (DWR) framework for deriving stopping criteria for iterative solvers used in the AFEM cycle. The DWR approach uses conventional residual-based error estimators for the iterate $\bar{u}_{\mathcal{T}}$, which is viewed as the exact solution to a perturbed problem: $a(\bar{u}_{\mathcal{T}}, v) = (f, v) - R(v)$, where $R(v)$ is the residual functional. The residual functional is estimated by the algebraic pointwise residual weighted by the inversion of the lumped mass matrix. The idea has been studied leading to various generalizations of the idea, it is extended to various other PDEs in [32]). Arioli et al ([3, 2, 1]) studied how to integrate these a posteriori error estimation techniques into an inexact AFEM cycle, as well as a stopping criteria using post-smoothed algebraic residuals from multiple levels.

Existing works using residual-based estimator on this topic focus mainly on the asymptotic regime for the given problem, where the superconvergence or the saturation assumption is exploited or assumed implicitly (e.g. see [4, 5]). Sufficient conditions for these properties normally require a certain regularity of the mesh, e.g., a sufficiently smooth mesh to resolve the data oscillation ([23]), or a mildly structured mesh ([35]). However, in the pre-asymptotic regime, where the discretization error $\|u - u_{\mathcal{T}}\|_A$ manifests itself in the total error $\|u - \bar{u}_{\mathcal{T}}\|_A$, such assumptions are too restrictive if the goal is to obtain sharp estimates when working in the pre-asymptotic regime.

In [27, 22], an equilibrated flux is used to construct an a posteriori error estimator for the iterate, which in our view is more suitable for the pre-asymptotic regime. For the

algebraic part of the error, the so-called "algebraic flux" is firstly obtained by taking the difference of the equilibrated fluxes between iterations. The algebraic error estimator is further constructed using this flux for the stopping criterion. In this approach, the algebraic error is not reconstructed on a given iteration.

In this paper, firstly, a locally post-processed flux based on the iterate $\bar{u}_{\mathcal{T}}$ is constructed using equilibration techniques. The construction we will follow is based on a local $H(\mathrm{div})$-lifting on vertex patches that has been studied by many researchers [9, 21, 29, 34, 16]. We note that due to the lack of the Galerkin orthogonality for the current iterate $\bar{u}_{\mathcal{T}}$, the overall construction used in these works needs to be modified. In particular, the global reliability of the error estimator follows naturally from the duality theory between the primary and the dual energy functionals to be minimized and maximized respectively (see Chapter 3 in [25]). The local efficiency proof mechanism requires the use of the inf-sup stability for a local hybridized-mixed problem, an idea that was developed in [16] and that we will follow. For the estimator proposed, the reliability bound is constant free, and the local efficiency constant is independent of the coefficient jump ratio under the quasi-monotonicy assumption for the distribution of the coefficient on a vertex patch.

Secondly, to construct the algebraic error estimator, the rate of the convergence of multigrid solver is approximated based on the algebraic residual of consecutive iterations. Then the algebraic error can be estimated using the fact that the rate of the convergence is the largest eigenvalue of the error propagation matrix of the iterative solver. The algebraic error estimator we propose bears similarity with the one in [27, 22], in that we both use the difference of the consecutive iterates measure in the energy norm. Moreover, we bridge the connection between the difference of the consecutive iterates and the algebraic error through the error propagation operator, and the reliability of the algebraic estimator is proved. Based on the algebraic estimator and the total error estimator, a stopping criterion for a given linear solver is proposed.

Lastly, in order to verify the efficiency of the new stopping criterion, we present numerical results for various types of test problems in Section 6.

2 Finite element method and multigrid solver

In this section all the preliminaries are presented. The following notation is adopted for the Sobolev space $H^1(\Omega)$ with a specified boundary value:

$$H^1_g(\Omega) := \{v \in H^1(\Omega) : \ v = g \ \text{ on } \ \partial\Omega\},$$

and $H^1_0(\Omega)$ is the zero Dirichlet boundary value subspace of $H^1_g(\Omega)$. The variational problem (1.1) is

$$\begin{cases} \text{Find } \ u \in H^1_g(\Omega) \ \text{ such that,} \\ \big(A\nabla u, \nabla v\big) = \big(f, v\big), \quad \forall v \in H^1_0(\Omega), \end{cases} \tag{2.1}$$

where and $\big(\cdot, \cdot\big)$ denotes the L^2-inner product on the whole domain.

Let $\mathcal{T} = \{K\}$ be a triangulation of Ω using simplicial elements. $\mathcal{T}$ is assumed to be quasi-uniform and regular. For each $K \in \mathcal{T}$, $h_K := \operatorname{diam}(K) = O(|K|^{1/d})$. The set of all the vertices of this triangulation is denoted by $\mathcal{N}$. Throughout this paper, the term "face" is used to refer the $(d-1)$-facet of an d-simplex in this triangulation $(d = 2, 3)$. For $d = 2$ case, face actually represents edge. The set of all the interior faces is denoted by $\mathcal{F}$. For any $F \in \mathcal{F}$, $h_F := \operatorname{diam}(F) = O(|F|^{1/(d-1)})$. Each face $F \in \mathcal{F}$ is assigned with a fixed unit normal $\boldsymbol{n}_F$ globally. For any function or distribution v well-defined on the two elements sharing a face F respectively, define $[\![v]\!]_F = v^- - v^+$ on an interior face. The v^- and v^+ are defined in the limiting sense $v^{\pm} = \lim\limits_{\epsilon \to 0^{\pm}} v(\boldsymbol{x} + \epsilon \boldsymbol{n}_F)$. If F is a boundary face, the function v is extended by zero outside the domain to compute $[\![v]\!]_F$. When $d = 2$, the clockwise rotation by $\pi/2$ from the original vector $\begin{pmatrix} a \\ b \end{pmatrix}$ is defined as $\begin{pmatrix} a \\ b \end{pmatrix}^{\perp} := \begin{pmatrix} b \\ -a \end{pmatrix}$.

For the purpose of constructing the local error estimation procedure for finite element approximation, the following local geometric objects notation are used in this paper. Firstly denote $\mathcal{N}_\omega$ as the vertices in $\bar{\omega}$. For any vertex $\boldsymbol{z} \in \mathcal{N}$, denote by

$$\omega_{\boldsymbol{z}} := \bigcup_{\{K \in \mathcal{T}:\, \boldsymbol{z} \in \mathcal{N}_K\}} K$$

as the vertex patch, which is the collection of all elements sharing $\boldsymbol{z}$ as a common vertex. Now $\mathcal{T}_{\boldsymbol{z}}$ stands for the triangulation of this patch such that $\mathcal{T}_{\boldsymbol{z}} := \{K : K \subset \omega_{\boldsymbol{z}}\}$. Denote

$$\omega_K := \bigcup_{\boldsymbol{z} \in \mathcal{N}_K} \omega_{\boldsymbol{z}}$$

as the element patch for K that contains all the elements sharing a vertex with K. Denote $\omega_{\boldsymbol{z}}^A$ as the coefficient A weighted patch:

$$\omega_{\boldsymbol{z}}^A := \bigcup_{\{K \subset \omega_{\boldsymbol{z}}:\, A_K = \max\limits_{K' \subset \omega_{\boldsymbol{z}}} A_{K'}\}} K.$$

For a face $F \in \mathcal{F}$, denote the face patch as

$$\omega_F := \bigcup_{F \cap \partial K \neq \emptyset} K,$$

which contains the elements sharing F as a common face. The L^2-inner product on $\omega_{\boldsymbol{z}}$ is denoted as $\big(\cdot, \cdot\big)_{\mathcal{T}_{\boldsymbol{z}}}$ requiring no inter-element continuity across interfaces: for $u|_K, v|_K \in L^2(K)$

$$\big(u,\, v\big)_{\mathcal{T}_{\boldsymbol{z}}} := \sum_{K \in \mathcal{T}_{\boldsymbol{z}}} (u, v)_K,$$

and this notation carries through for the vector-valued functions. The following norms for a function are used throughout this paper:

$$\|v\|_{0,\omega}^2 := (v, v)_\omega \ \text{ and } \ \|v\|_{1,\omega}^2 := \big(\nabla v,\, \nabla v\big)_\omega + \big(v,\, v\big)_\omega, \tag{2.2}$$

and if the subscript is dropped, $\omega = \Omega$. The "energy" norm associated with the problem (2.1) is:

$$\|v\|_A^2 := \big(A\nabla u,\, \nabla v\big), \quad \text{and} \quad \|v\|_{A,\omega}^2 := \big(A\nabla u,\, \nabla v\big)_\omega. \tag{2.3}$$

Let $\mathcal{F}_K$ be the set of faces of an element $K \in \mathcal{T}$. Denote the set of the interior faces within $\omega_{\boldsymbol{z}}$ as:

$$\mathcal{F}_{\boldsymbol{z}} := \{F \in \mathcal{F} : F \in \mathcal{F}_K \text{ for } K \subset \omega_{\boldsymbol{z}},\ F \cap \partial\omega_{\boldsymbol{z}} = \emptyset\}.$$

For u, v well-defined on each face $F \in \mathcal{F}_{\boldsymbol{z}}$ such that $u\big|_F \in L^2(F)$ and $v\big|_F \in L^2(F)$, the following inner product notation is adopted:

$$\big(u,\, v\big)_{\mathcal{F}_{\boldsymbol{z}}} := \sum_{F\in\mathcal{F}_{\boldsymbol{z}}} \big(u\big|_F,\, v\big|_F\big)_F.$$

The finite element approximation to problem (2.1) uses the the linear Lagrange elements which is H^1-conforming on the triangulation:

$$\mathcal{S}_\mathcal{T} := \{v \in H^1(\Omega) :\, v\big|_K \in P_1(K), \quad \text{for } \forall K \in \mathcal{T}\}, \tag{2.4}$$

The finite element approximation problem to (2.1) is then

$$\begin{cases} \text{Find} \quad u_\mathcal{T} \in \mathcal{S}_{\mathcal{T},g} := \mathcal{S}_\mathcal{T} \cap H^1_g(\Omega) \quad \text{such that,} \\ \big(A\nabla u_\mathcal{T},\, \nabla v\big) = \big(f,\, v\big), \quad \forall v \in \mathcal{S}_{\mathcal{T},0}. \end{cases} \tag{2.5}$$

For the presentation purpose, here it is assumed that both the diffusion coefficient $A\big|_K = A_K$ and the data $f\big|_K = f_K$ are piecewise constants with respect to the triangulation $\mathcal{T}$, and the Dirichlet boundary data g can be represented by the trace of a function in $\mathcal{S}_\mathcal{T}$. In this setting, no data oscillation term will be present in the final error estimate bounds.

Provided that the problem (2.5) is assembled using the the nodal basis function for (2.4), i.e. $\phi_{\boldsymbol{z}_i}$ being the Lagrange nodal basis function of $\mathcal{S}_\mathcal{T}$ associated with an interior vertex $\boldsymbol{z}_i$ in this triangulation. An iterative solver shall be used to approximate the following linear system:

$$\mathbf{A}\mathbf{u} = \mathbf{f}. \tag{2.6}$$

The stiffness matrix $\mathbf{A}$ associated with problem (2.5) is $\mathbf{A}[i,j] = a_{ij}$, where $a_{ij} = \big(A\nabla\phi_{\boldsymbol{z}_j},\, \nabla\phi_{\boldsymbol{z}_i}\big)$. $\mathbf{u}$ is the vector representation of the exact solution $u_\mathcal{T}$ of the discretized problem. $\mathbf{f}$ is the vector representation of the right hand side of problem (2.5), with i-th row $\mathbf{f}[i]$ of $\mathbf{f}$ is $(f, \phi_{\boldsymbol{z}_i})$. Instead of applying a direct solver such as `MATLAB`'s built-in `linsolve`, the multilevel hierarchy of finite element spaces on coarse and fine meshes is exploited to build a more efficient iterative multigrid solver (e.g. see [11]). Let $\mathbf{u}^{(k)}$ be the vector representation of the k-th iterate $u_\mathcal{T}^{(k)}$ in the nodal basis.

Provided that the iterative solver is linear and symmetric (such as a full multigrid, a single multigrid V-cycle, or forward-backward Gauss-Seidel sweepings), and is associated with a symmetric iterator matrix $\mathbf{B}$, one iteration of the solver, for the linear

system (2.6) can be represented as follows. Given the current iterate $\mathbf{u}^{(k)}$, the following operation yields the the new iterate $\mathbf{u}^{(k+1)}$ as the output:

$$\mathbf{u}^{(k+1)} = \mathbf{u}^{(k)} + \mathbf{B}(\mathbf{f} - \mathbf{A}\mathbf{u}^{(k)}), \tag{2.7}$$

and let the corresponding function in the finite element space be $u_{\mathcal{T}}^{(k+1)}$. Here $k \geq 0$, with $\mathbf{u}^{(0)}$ being the initial guess.

Next we define the norms for vectors and matrices: with the help of the context, the usual 2-norm $\|\cdot\|_2$ for a vector $\mathbf{v} \in \mathbb{R}^n$ and a non-singular square matrix $\mathbf{M} \in \mathbb{R}^{n\times n}$ is defined by:

$$\|\mathbf{v}\|_2 := \sqrt{\mathbf{v}\cdot\mathbf{v}}, \text{ and } \|\mathbf{M}\|_2 := \sup_{\|\mathbf{v}\|_2=1} \|\mathbf{M}\mathbf{v}\|_2 = \rho(\mathbf{M}), \tag{2.8}$$

where $\rho(\mathbf{M})$ is the spectral radius of $\mathbf{M}$ equaling its largest eigenvalue.

Due to the fact that we opt for the Dirichlet boundary condition, the stiffness matrix $\mathbf{A}$ is symmetric positive definite. As a result, $\mathbf{A}^{1/2}$ is non-singular and can be used to induce a norm:

$$\|\mathbf{v}\|_{\mathbf{A}} := \sqrt{\mathbf{A}\mathbf{v}\cdot\mathbf{v}} = \left\|\mathbf{A}^{1/2}\mathbf{v}\right\|_2, \text{ and } \|\mathbf{M}\|_{\mathbf{A}} := \sup_{\|\mathbf{v}\|_{\mathbf{A}}=1} \|\mathbf{M}\mathbf{v}\|_{\mathbf{A}}. \tag{2.9}$$

By definition it is straightforward to verify that:

$$\|\mathbf{M}\|_{\mathbf{A}} = \sup_{\left\|\mathbf{A}^{1/2}\mathbf{v}\right\|_2=1} \left\|\mathbf{A}^{1/2}\mathbf{M}\mathbf{v}\right\|_2 = \left\|\mathbf{A}^{1/2}\mathbf{M}\mathbf{A}^{-1/2}\right\|_2. \tag{2.10}$$

For a finite element function v and its vector representation $\mathbf{v}$, the following equivalence between vector norm and Sobolev norm holds as well:

$$\|v\|_A = \|\mathbf{v}\|_{\mathbf{A}}. \tag{2.11}$$

3 A posteriori error estimation using equilibrated flux

In this section, firstly the duality theory for error estimation is introduced. Then a locally post-processed flux based on the iterate $\bar{u}_{\mathcal{T}}$ is constructed. Lastly the reliability and efficiency of the estimator based on this flux is proved.

3.1 Duality theory

It is known that the variational problem in (2.1) can be rewritten as a functional minimization problem, where the primal functional is defined as:

$$\mathcal{J}(v) := \frac{1}{2}\left(A\nabla v, \nabla v\right) - \left(f, v\right) \tag{3.1}$$

Then the primal problem is equivalent to the following minimization problem:

$$\text{Find } u \in H_g^1(\Omega) \text{ such that } \mathcal{J}(u) = \min_{v\in H_g^1(\Omega)} \mathcal{J}(v). \tag{3.2}$$

The dual functional with respect to (3.1) is:

$$\mathcal{J}^*(\boldsymbol{\tau}) := -\frac{1}{2}\big(A^{-1}\boldsymbol{\tau},\, \boldsymbol{\tau}\big). \tag{3.3}$$

The dual problem is then to maximize $\mathcal{J}^*(\boldsymbol{\tau})$, in the following suitable space:

$$\boldsymbol{\Sigma} := \{\boldsymbol{\tau} \in \boldsymbol{H}(\mathrm{div};\Omega) :\ \nabla\cdot\boldsymbol{\tau} = f\}. \tag{3.4}$$

Now the dual problem can be phrased as:

$$\text{Find } \boldsymbol{\sigma} \in \boldsymbol{\Sigma} \ \text{ such that } \ \mathcal{J}^*(\boldsymbol{\sigma}) = \max_{\boldsymbol{\tau}\in\boldsymbol{\Sigma}} \mathcal{J}^*(\boldsymbol{\tau}). \tag{3.5}$$

The foundation to use the dual problem in constructing a posteriori error estimator is that the minimum of the primal functional $\mathcal{J}(\cdot)$ coincides with the maximum of the dual functional $\mathcal{J}^*(\boldsymbol{\sigma})$ (see [25] Chapter 3):

$$\mathcal{J}(u) = \mathcal{J}^*(\boldsymbol{\sigma}), \ \text{ and that } \ \boldsymbol{\sigma} = -A\nabla u. \tag{3.6}$$

Now that (3.6) is satisfied, then a guaranteed upper bound can be obtained as follows: for any $\boldsymbol{\sigma}_{\mathcal{T}} \in \boldsymbol{\Sigma}_{\mathcal{T}} := \boldsymbol{\Sigma} \cap \boldsymbol{\mathcal{RT}}^0$

$$\begin{aligned} \|u - \bar{u}_{\mathcal{T}}\|_A^2 &= 2\Big(\mathcal{J}(\bar{u}_{\mathcal{T}}) - \mathcal{J}(u)\Big) \\ &= 2\Big(\mathcal{J}(\bar{u}_{\mathcal{T}}) - \mathcal{J}^*(\boldsymbol{\sigma})\Big) \le 2\Big(\mathcal{J}(\bar{u}_{\mathcal{T}}) - \mathcal{J}^*(\boldsymbol{\sigma}_{\mathcal{T}})\Big). \end{aligned} \tag{3.7}$$

One of the main goals of this paper is to locally construct such $\boldsymbol{\sigma}_{\mathcal{T}}$ based on the current iterative solver output $\bar{u}_{\mathcal{T}}$, that the global reliability bound (3.7) is automatically met with the local efficiency bound (locally the energy error is bounded above by the estimator) being satisfied as well.

3.2 Localized flux recovery

Let $\boldsymbol{\sigma}^{\Delta}$ be the correction from $-A\nabla\bar{u}_{\mathcal{T}}$ to the true $\boldsymbol{\sigma} := -A\nabla u$:

$$\boldsymbol{\sigma}^{\Delta} := \boldsymbol{\sigma} - \big(-A\nabla\bar{u}_{\mathcal{T}}\big) \tag{3.8}$$

Let $\boldsymbol{\sigma}^{\Delta}$ be decomposed using a partition of unity $\{\phi_{\boldsymbol{z}}\}_{\boldsymbol{z}\in\mathcal{N}}$, which is the set of the nodal basis functions for the linear Lagrange element space $\mathcal{S}_{\mathcal{T}}$:

$$\boldsymbol{\sigma}^{\Delta} = \sum_{\boldsymbol{z}\in\mathcal{N}} \boldsymbol{\sigma}_{\boldsymbol{z}}^{\Delta}, \ \text{ with } \boldsymbol{\sigma}_{\boldsymbol{z}}^{\Delta} := \phi_{\boldsymbol{z}}\boldsymbol{\sigma}^{\Delta}. \tag{3.9}$$

The local problem for $\boldsymbol{\sigma}_{\boldsymbol{z}}^{\Delta}$ satisfies is as follows: On the element $K \subset \omega_{\boldsymbol{z}}$,

$$\begin{cases} \nabla\cdot\boldsymbol{\sigma}_{\boldsymbol{z}}^{\Delta} = \phi_{\boldsymbol{z}}\bar{r}_K - \nabla\phi_{\boldsymbol{z}}\cdot\nabla(u-\bar{u}_{\mathcal{T}}), & \text{on } K \subset \omega_{\boldsymbol{z}}, \\ [\![\boldsymbol{\sigma}_{\boldsymbol{z}}^{\Delta}\cdot\boldsymbol{n}_F]\!]_F = \phi_{\boldsymbol{z}}\bar{j}_F, & \text{on } F \in \mathcal{F}_{\boldsymbol{z}} \text{ or } F \subset \partial\Omega, \\ \boldsymbol{\sigma}_{\boldsymbol{z}}^{\Delta}\cdot\boldsymbol{n}_F = 0, & \text{on } F \subset \partial\omega_{\boldsymbol{z}}\backslash\partial\Omega, \end{cases} \tag{3.10}$$

where the element residual $\bar{r}_K$ for $\bar{u}_{\mathcal{T}}$ on an element K is:

$$\bar{r}_K := \left\{ f + \nabla\cdot(A\nabla\bar{u}_{\mathcal{T}}) \right\}\big|_K = f\big|_K = f_K,$$

and this is a constant in K. The normal jump of $\bar{u}_{\mathcal{T}}$ on the face F is:

$$\bar{j}_F := -[\![A\nabla(u-\bar{u}_{\mathcal{T}})\cdot\boldsymbol{n}_F]\!]_F = \begin{cases} [\![A\nabla\bar{u}_{\mathcal{T}}\cdot\boldsymbol{n}_F]\!]_F, & \text{if } F\in\mathcal{F}_{\boldsymbol{z}}, \\ A\nabla(u-\bar{u}_{\mathcal{T}})\cdot\boldsymbol{n}_F, & \text{if } F\subset\partial\Omega. \end{cases}$$

which is constant F if F is an interior face. To approximate problem (3.10), an approximated correction flux $\boldsymbol{\sigma}^{\Delta}_{\boldsymbol{z},\mathcal{T}}$ is sought in the following broken lowest-order Raviart-Thomas space:

$$\boldsymbol{\mathcal{RT}}^0_{-1,\omega_{\boldsymbol{z}}} := \left\{ \boldsymbol{\tau}\in\boldsymbol{L}^2(\omega_{\boldsymbol{z}}) : \boldsymbol{\tau}\big|_K \in \boldsymbol{\mathcal{RT}}^0(K),\ \forall K\subset\omega_{\boldsymbol{z}} \right\}. \tag{3.11}$$

This $\boldsymbol{\sigma}^{\Delta}_{\boldsymbol{z},\mathcal{T}}$ is firstly constructed through an explicit procedure, usually named by equilibration (see [8, 9]), satisfying the following problem:

$$\begin{cases} \nabla\cdot\boldsymbol{\sigma}^{\Delta}_{\boldsymbol{z},\mathcal{T}} = \bar{r}_{K,\boldsymbol{z}} + \alpha_{K,\boldsymbol{z}}c_{\boldsymbol{z}}, & \text{on } K\subset\omega_{\boldsymbol{z}}, \\ [\![\boldsymbol{\sigma}^{\Delta}_{\boldsymbol{z},\mathcal{T}}\cdot\boldsymbol{n}_F]\!]_F = \bar{j}_{F,\boldsymbol{z}}, & \text{on } F\in\mathcal{F}_{\boldsymbol{z}}, \\ \boldsymbol{\sigma}^{\Delta}_{\boldsymbol{z},\mathcal{T}}\cdot\boldsymbol{n}_F = 0, & \text{on } F\subset\partial\omega_{\boldsymbol{z}}\backslash\partial\Omega, \end{cases} \tag{3.12}$$

where $\bar{r}_{K,\boldsymbol{z}}$ and $\bar{j}_{F,\boldsymbol{z}}$ are defined as the L^2-projection of $\phi_{\boldsymbol{z}}\bar{r}_K$ and $\phi_{\boldsymbol{z}}\bar{j}_F$ onto the constant space of K and interior F respectively:

$$\begin{aligned} \bar{r}_{K,\boldsymbol{z}} &:= \Pi_K(\phi_{\boldsymbol{z}}\bar{r}_K) = \frac{1}{d+1}f_K = \frac{1}{d+1}\bar{r}_K, \\ \bar{j}_{F,\boldsymbol{z}} &:= \Pi_F(\phi_{\boldsymbol{z}}\bar{j}_F) = \frac{1}{d}[\![(A\nabla\bar{u}_{\mathcal{T}})\cdot\boldsymbol{n}_F]\!]_F = \frac{1}{d}\bar{j}_F. \end{aligned} \tag{3.13}$$

Moreover, the element-wise added compensation term $c_{\boldsymbol{z}}$, which is a constant for this vertex patch $\omega_{\boldsymbol{z}}$, is:

$$c_{\boldsymbol{z}} := \frac{1}{|\omega_{\boldsymbol{z}}|}\Big(\big(\bar{j}_{F,\boldsymbol{z}},\,1\big)_{\mathcal{F}_{\boldsymbol{z}}} - \big(\bar{r}_{K,\boldsymbol{z}},\,1\big)_{\mathcal{T}_{\boldsymbol{z}}} \Big). \tag{3.14}$$

We noted that if $\bar{u}_{\mathcal{T}}$ solves the discretized finite element system exactly, $c_{\boldsymbol{z}} = 0$, and this is called Galerkin orthogonality. The existence of the discrete divergence problem (3.12) relies on the Galerkin orthogonality (see [9, 16]). Here, $c_{\boldsymbol{z}}$ is added to remedy the violation of the Galerkin orthogonality by (a) $\bar{u}_{\mathcal{T}}$ on this patch $\omega_{\boldsymbol{z}}$, which is not the exact finite element approximation, and (b) the nodal basis $\phi_{\boldsymbol{z}}$ associated with a boundary vertex $\boldsymbol{z}$ not being in the test function space. The weight $\alpha_{K,\boldsymbol{z}}$ is a piecewise constant on the patch $\omega_{\boldsymbol{z}}$ such that

$$\alpha_{K,\boldsymbol{z}} = \begin{cases} |\omega_{\boldsymbol{z}}|/|\omega^A_{\boldsymbol{z}}|, & \text{if } K\subset\omega^A_{\boldsymbol{z}}, \\ 0, & \text{if } K\subset\omega_{\boldsymbol{z}}\backslash\omega^A_{\boldsymbol{z}}. \end{cases} \tag{3.15}$$

The shape regularity of the triangulation $\mathcal{T}$ guarantees that $1 \leq \alpha_{K,\boldsymbol{z}} \leq \dim \mathcal{T}_{\boldsymbol{z}} < \infty$ if $K \subset \omega_{\boldsymbol{z}}^A$.

Then the flux correction is postprocessed by a minimization procedure:

$$\left\| A^{-1/2} \boldsymbol{\sigma}_{\boldsymbol{z},\mathcal{T}}^{\Delta} \right\|_{0,\omega_{\boldsymbol{z}}} = \min_{\boldsymbol{\tau} \in \boldsymbol{\Sigma}_{\boldsymbol{z},\mathcal{T}}} \left\| A^{-1/2} \boldsymbol{\tau} \right\|_{0,\omega_{\boldsymbol{z}}}, \tag{3.16}$$

where $\boldsymbol{\Sigma}_{\boldsymbol{z},\mathcal{T}} := \left\{ \boldsymbol{\tau} \in \boldsymbol{\mathcal{RT}}^0_{-1,\omega_{\boldsymbol{z}}} : \boldsymbol{\tau} \text{ satisfies (3.12)} \right\}$. The element-wise and the global flux corrections are then:

$$\boldsymbol{\sigma}_{K,\mathcal{T}}^{\Delta} := \sum_{\boldsymbol{z} \in \mathcal{N}_K} \boldsymbol{\sigma}_{\boldsymbol{z},\mathcal{T}}^{\Delta}, \quad \text{and} \quad \boldsymbol{\sigma}_{\mathcal{T}}^{\Delta} := \sum_{\boldsymbol{z} \in \mathcal{N}} \boldsymbol{\sigma}_{\boldsymbol{z},\mathcal{T}}^{\Delta}. \tag{3.17}$$

Lastly, a globally defined term $\boldsymbol{\sigma}_{\mathcal{T}}^c$ is as follows: seeking $\boldsymbol{\sigma}_{\mathcal{T}}^c$ in the global $\boldsymbol{\mathcal{RT}}^0$ space

$$\nabla \cdot \boldsymbol{\sigma}_{\mathcal{T}}^c = - \sum_{\boldsymbol{z} \in \mathcal{N}_K} \alpha_{K,\boldsymbol{z}} c_{\boldsymbol{z}} =: f_c \quad , \text{ in any } K \in \mathcal{T}, \tag{3.18}$$

then denote $\boldsymbol{\sigma}_{K,\mathcal{T}}^c := \boldsymbol{\sigma}_{\mathcal{T}}^c\big|_K$. By the surjectivity of the divergence operator from $\boldsymbol{\mathcal{RT}}^0$ to the piecewise constant, above problem has a solution. If $\boldsymbol{\sigma}_{\mathcal{T}}^c$ is sought using minimizing the L^2-norm, with (3.18) being a constraint. It is equivalent to seeking the solution to a mixed finite element problem, and $\boldsymbol{\sigma}_{\mathcal{T}}^c$ satisfies the energy estimate in L^2 norm (see e.g. [10, 19]):

$$\|\boldsymbol{\sigma}_{\mathcal{T}}^c\|_0 \leq \|f_c\|_{-1,\mathcal{T}} \leq \left\{ \sum_{K \in \mathcal{T}} h_K^2 \|f_c\|_{0,K} \right\}^{1/2}. \tag{3.19}$$

$\boldsymbol{\sigma}_{\mathcal{T}}^c$ is here to compensate the change caused by the correction term $c_{\boldsymbol{z}}$. $\boldsymbol{\sigma}_{K,\mathcal{T}}^c$ will not be constructed explicitly. The explicit constructions of $\boldsymbol{\sigma}_{\boldsymbol{z},\mathcal{T}}^{\Delta}$ will be presented in Section 5.

The recovered flux based on the $\bar{u}_{\mathcal{T}}$ is defined as:

$$\boldsymbol{\sigma}_{\mathcal{T}} := -A \nabla \bar{u}_{\mathcal{T}} + \boldsymbol{\sigma}_{\mathcal{T}}^{\Delta} + \boldsymbol{\sigma}_{\mathcal{T}}^c, \tag{3.20}$$

while in practice only $\boldsymbol{\sigma}_{\mathcal{T}}^{\Delta}$ is explicitly computed.

Lemma 3.1. *The recovered flux $\boldsymbol{\sigma}_{\mathcal{T}}$ is in the conforming finite element subspace of the duality space: $\boldsymbol{\sigma}_{\mathcal{T}} \in \boldsymbol{\Sigma}_{\mathcal{T}} := \boldsymbol{\Sigma} \cap \boldsymbol{\mathcal{RT}}^0$.*

Proof. In any element K:

$$\nabla \cdot \boldsymbol{\sigma}_{\mathcal{T}}\big|_K = \nabla \cdot \left(-A \nabla \bar{u}_{\mathcal{T}} + \boldsymbol{\sigma}_{\mathcal{T}}^{\Delta} + \boldsymbol{\sigma}_{\mathcal{T}}^c \right) = \nabla \cdot \boldsymbol{\sigma}_{\mathcal{T}}^{\Delta} + \nabla \cdot \boldsymbol{\sigma}_{\mathcal{T}}^c,$$

Using (3.12) and (3.18), together with the fact that $A \nabla \bar{u}_{\mathcal{T}}$ is a constant vector on each element K, we have:

$$\nabla \cdot \boldsymbol{\sigma}_{\mathcal{T}}\big|_K = \nabla \cdot \boldsymbol{\sigma}_{\mathcal{T}}^{\Delta} + \nabla \cdot \boldsymbol{\sigma}_{\mathcal{T}}^c = \sum_{\boldsymbol{z} \in \mathcal{N}_K} \bar{r}_{K,\boldsymbol{z}} = f_K.$$

On any interior face F, using the fact that $[\![\boldsymbol{\sigma}_{\mathcal{T}}^{c}\cdot\boldsymbol{n}]\!]_F=0$ due to $\boldsymbol{\sigma}_{\mathcal{T}}^{c}\in\boldsymbol{H}(\mathrm{div};\Omega)$:

$$[\![\boldsymbol{\sigma}_{\mathcal{T}}\cdot\boldsymbol{n}]\!]_F=[\![\boldsymbol{\sigma}_{\mathcal{T}}^{\Delta}\cdot\boldsymbol{n}]\!]_F-[\![A\nabla\bar{u}_{\mathcal{T}}\cdot\boldsymbol{n}]\!]_F=\sum_{\boldsymbol{z}\in\mathcal{N}(F)}\bar{j}_{F,\boldsymbol{z}}-\bar{j}_F=0.$$

□

The global error estimator and local error indicator based on the flux corrections (3.17) are defined as:

$$\begin{aligned}\eta_{D,\boldsymbol{z}}:=\left\|A^{-1/2}\boldsymbol{\sigma}_{\boldsymbol{z},\mathcal{T}}^{\Delta}\right\|_{0,\omega_{\boldsymbol{z}}},\quad \eta_{D,K}:=\left\|A^{-1/2}\boldsymbol{\sigma}_{K,\mathcal{T}}^{\Delta}\right\|_{0,K},\\ \text{and}\quad \eta_D:=\left\|A^{-1/2}\boldsymbol{\sigma}_{\mathcal{T}}^{\Delta}\right\|_{0}.\end{aligned}\tag{3.21}$$

3.3 Reliability and efficiency for the total error estimator

The reliability we show in this section is: the total error $\|u-\bar{u}_{\mathcal{T}}\|_A$ is bounded by the total error estimator plus the algebraic error. We show the efficiency by proving that every component of error estimator locally can be bounded by the total error $\|u-\bar{u}_{\mathcal{T}}\|_{A,\omega_{\boldsymbol{z}}}$ within a given vertex patch $\omega_{\boldsymbol{z}}$.

In order that the constants in the a posteriori error bounds are independent of the coefficients, the following assumptions are needed. First assumption is the quasi-monotonicity of the coefficient distribution, it is commonly used in obtaining a robust a posteriori error bound for interface problem introduced firstly in [24]. The interpolation estimates for elliptic interface problems are further discussed in [31, 7]. The second assumption is a common practice in the error analysis of Discontinuous Galerkin (DG) finite elements (see [15]), and here we use this assumption to prove the local error estimates for the correction term on a boundary vertex patch.

Assumption 3.2 (Quasi-monotonicity assumption or QMA)**.** *For any two different element K_i and K_j in a vertex patch $\omega_{\boldsymbol{z}}$, there is a connected path passing through adjacent elements $K_l\subset\omega_{\boldsymbol{z}}$ ($l\in\{1,\cdots,N_{\boldsymbol{z}}\}$) sharing at least a face, such that the coefficient A_l is monotone along this path.*

Assumption 3.3 (Regularity assumption)**.** *The weak solution u to the problem (2.1) is in the following space: there exist a fixed $\epsilon>0$*

$$u\in\{v\in H^{1+\epsilon}(\Omega):\ \nabla\cdot(A\nabla v)\in L^2(K),\ \forall K\in\mathcal{T}\}.\tag{3.22}$$

Lemma 3.4 (Nodal residual estimate)**.** *The Galerkin orthogonality compensation term $c_{\boldsymbol{z}}$ satisfies the following L^2-estimate in $K\subset\omega_{\boldsymbol{z}}$: for any interior vertex $\boldsymbol{z}\in\mathcal{N}_K$,*

$$\begin{aligned}\|c_{\boldsymbol{z}}\|_{0,K}\le C_1\,h_K^{-1}\Big(\max_{K\subset\omega_{\boldsymbol{z}}}A_K^{1/2}\Big)\,\|u-\bar{u}_{\mathcal{T}}\|_{A,\omega_{\boldsymbol{z}}},\\ \textit{and}\ \ \|c_{\boldsymbol{z}}\|_{0,K}\le C_2\,h_K^{-1}\Big(\max_{K\subset\omega_{\boldsymbol{z}}}A_K^{1/2}\Big)\,\|u_{\mathcal{T}}-\bar{u}_{\mathcal{T}}\|_{A,\omega_{\boldsymbol{z}}}.\end{aligned}\tag{3.23}$$

For any boundary vertex $\boldsymbol{z} \in \mathcal{N}_K$,

$$\|c_{\boldsymbol{z}}\|_{0,K} \leq C_3\, h_K^{-1}\Big(\max_{K\subset\omega_{\boldsymbol{z}}} A_K^{1/2}\Big) \sum_{K\subset\omega_{\boldsymbol{z}}} \Big(\|u-\bar{u}_{\mathcal{T}}\|_{A,K} + A_K^{-1/2}\,\|\bar{r}_K\|_{0,K}\Big)\,. \tag{3.24}$$

Proof. First for any interior vertex $\boldsymbol{z}$, it can be observed that $c_{\boldsymbol{z}}$ in (3.14) is the algebraic residual for the test function $\phi_{\boldsymbol{z}}$ weighted by the patch area:

$$\begin{aligned} c_{\boldsymbol{z}}|\omega_{\boldsymbol{z}}| &= \big(\bar{j}_{F,\boldsymbol{z}},\,1\big)_{\mathcal{F}_{\boldsymbol{z}}} - \big(\bar{r}_{K,\boldsymbol{z}},\,1\big)_{\mathcal{T}_{\boldsymbol{z}}} \\ &= \big(\bar{j}_F,\,\phi_{\boldsymbol{z}}\big)_{\mathcal{F}_{\boldsymbol{z}}} - \big(\bar{r}_K,\,\phi_{\boldsymbol{z}}\big)_{\mathcal{T}_{\boldsymbol{z}}} = \big(A\nabla(u-\bar{u}_{\mathcal{T}}),\,\nabla\phi_{\boldsymbol{z}}\big)_{\mathcal{T}_{\boldsymbol{z}}}. \end{aligned} \tag{3.25}$$

Applying Cauchy-Schwarz inequality:

$$|c_{\boldsymbol{z}}| = \frac{1}{|\omega_{\boldsymbol{z}}|}\Big|\big(A\nabla(u-\bar{u}_{\mathcal{T}}),\,\nabla\phi_{\boldsymbol{z}}\big)_{\mathcal{T}_{\boldsymbol{z}}}\Big| \leq \frac{1}{|\omega_{\boldsymbol{z}}|}\,\|u-\bar{u}_{\mathcal{T}}\|_{A,\omega_{\boldsymbol{z}}}\,\|\phi_{\boldsymbol{z}}\|_{A,\omega_{\boldsymbol{z}}}\,.$$

By $\|\nabla\phi_{\boldsymbol{z}}\|_{0,K} \leq C\,h_K^{\frac{d}{2}-1}$, and using the shape regularity of the patch,

$$|c_{\boldsymbol{z}}| \leq C\,h_K^{-\frac{d}{2}-1}\Big(\max_{K\subset\omega_{\boldsymbol{z}}} A_K^{1/2}\Big)\,\|u-\bar{u}_{\mathcal{T}}\|_{A,\omega_{\boldsymbol{z}}}\,.$$

Lastly, the fact that $c_{\boldsymbol{z}}$ is a constant implies $\|c_{\boldsymbol{z}}\|_{0,K} \leq h_K^{\frac{d}{2}}\,|c_{\boldsymbol{z}}|$. Thus the estimate (3.23) holds.

Moreover, by Galerkin orthogonality, for any interior vertex $\boldsymbol{z}$:

$$\big(A\nabla(u-u_{\mathcal{T}}),\,\nabla\phi_{\boldsymbol{z}}\big)_{\mathcal{T}_{\boldsymbol{z}}} = 0.$$

Inserting this into (3.25), we have

$$c_{\boldsymbol{z}} = \frac{1}{|\omega_{\boldsymbol{z}}|}\big(A\nabla(u_{\mathcal{T}}-\bar{u}_{\mathcal{T}}),\,\nabla\phi_{\boldsymbol{z}}\big)_{\mathcal{T}_{\boldsymbol{z}}}.$$

Repeating above argument leads to the second estimate in (3.23).

Now for a vertex $\boldsymbol{z} \in \partial\Omega$, performing the integrating parts on each $K \subset \omega_z$, and the estimate (3.25) becomes

$$c_{\boldsymbol{z}} = \frac{1}{|\omega_{\boldsymbol{z}}|}\left[\big(A\nabla(u-\bar{u}_{\mathcal{T}}),\,\nabla\phi_{\boldsymbol{z}}\big)_{\mathcal{T}_{\boldsymbol{z}}} - \sum_{F\subset\partial\omega_{\boldsymbol{z}}\cap\partial\Omega}\langle A\nabla(u-\bar{u}_{\mathcal{T}})\cdot\boldsymbol{n},\phi_{\boldsymbol{z}}\rangle_F\right].$$

The first term can be estimated exactly the same with the (3.23). For the second term: for any boundary face F, by Assumption 3.3 and Lemma 2.4 in [17]

$$\begin{aligned} &\langle A\nabla(u-\bar{u}_{\mathcal{T}})\cdot\boldsymbol{n},\phi_{\boldsymbol{z}}\rangle_F \\ \leq\, & C\,h_K^{-1}\,\|\phi_{\boldsymbol{z}}\|_{0,K}\left(A_K^{1/2}\Big\|A^{1/2}\nabla(u-\bar{u}_{\mathcal{T}})\Big\|_{0,K} + \big\|\nabla\cdot\big(A\nabla(u-\bar{u}_{\mathcal{T}})\big)\big\|_{0,K}\right) \\ \leq\, & C\,h_K^{-1+\frac{d}{2}}A_K^{1/2}\Big(\|u-\bar{u}_{\mathcal{T}}\|_{A,K} + A_K^{-1/2}\,\|\bar{r}_K\|_{0,K}\Big)\,. \end{aligned}$$

Lastly applying the same argument to obtain (3.23) yields (3.24). □

Theorem 3.5 (Reliability of the total error estimator)**.** *The global error estimator* $\eta(\bar{u}_\mathcal{T})$ *is reliable in the following sense:*

$$\|u - \bar{u}_\mathcal{T}\|_A \leq \eta_D + C_A \|u_\mathcal{T} - \bar{u}_\mathcal{T}\|_A . \tag{3.26}$$

where the reliability constant for the discretization part is 1, and the algebraic part constant C_A *depends on* $(\max_{K\subset\omega_{\boldsymbol{z}}} A_K)/(\min_{K\subset\omega_{\boldsymbol{z}}} A_K)$*.*

Proof. The reliability bound proof starts from (3.7)

$$2\Big(\mathcal{J}(\bar{u}_\mathcal{T}) - \mathcal{J}^*(\boldsymbol{\sigma}_\mathcal{T})\Big) = \big(A\nabla\bar{u}_\mathcal{T},\, \nabla\bar{u}_\mathcal{T}\big) - 2\big(f,\, \bar{u}_\mathcal{T}\big) + \big(A^{-1}\boldsymbol{\sigma}_\mathcal{T},\, \boldsymbol{\sigma}_\mathcal{T}\big).$$

Evaluating the last term above using (3.20):

$$\begin{aligned}\big(A^{-1}\boldsymbol{\sigma}_\mathcal{T},\, \boldsymbol{\sigma}_\mathcal{T}\big) &= \big(A^{-1}(\boldsymbol{\sigma}_\mathcal{T}^\Delta + \boldsymbol{\sigma}_\mathcal{T}^c - A\nabla\bar{u}_\mathcal{T}),\, \boldsymbol{\sigma}_\mathcal{T}^\Delta + \boldsymbol{\sigma}_\mathcal{T}^c - A\nabla\bar{u}_\mathcal{T}\big)\\ &= \Big\|A^{-1/2}(\boldsymbol{\sigma}_\mathcal{T}^\Delta + \boldsymbol{\sigma}_\mathcal{T}^c)\Big\|_0^2 + \Big\|A^{1/2}\nabla\bar{u}_\mathcal{T}\Big\|_0^2 - 2\big(\boldsymbol{\sigma}_\mathcal{T}^\Delta + \boldsymbol{\sigma}_\mathcal{T}^c,\, \nabla\bar{u}_\mathcal{T}\big).\end{aligned}$$

Inserting back into the first equation, and performing integration by parts on the last term element-wisely:

$$\begin{aligned}&2\Big(\mathcal{J}(\bar{u}_\mathcal{T}) - \mathcal{J}^*(\boldsymbol{\sigma}_\mathcal{T})\Big)\\ &= \Big\|A^{-1/2}(\boldsymbol{\sigma}_\mathcal{T}^\Delta + \boldsymbol{\sigma}_\mathcal{T}^c)\Big\|_0^2 + 2\big(A\nabla\bar{u}_\mathcal{T} - \boldsymbol{\sigma}_\mathcal{T}^\Delta - \boldsymbol{\sigma}_\mathcal{T}^c,\, \nabla\bar{u}_\mathcal{T}\big) - 2\big(f,\, \bar{u}_\mathcal{T}\big)\\ &= \Big\|A^{-1/2}(\boldsymbol{\sigma}_\mathcal{T}^\Delta + \boldsymbol{\sigma}_\mathcal{T}^c)\Big\|_0^2 + 2\sum_{K\in\mathcal{T}}\big(\nabla\cdot(\boldsymbol{\sigma}_\mathcal{T}^\Delta + \boldsymbol{\sigma}_\mathcal{T}^c - A\nabla\bar{u}_\mathcal{T}),\, \bar{u}_\mathcal{T}\big)_K\\ &\quad + 2\sum_{F\in\mathcal{F}}\big([\![(\boldsymbol{\sigma}_\mathcal{T}^\Delta + \boldsymbol{\sigma}_\mathcal{T}^c - A\nabla\bar{u}_\mathcal{T})\cdot\boldsymbol{n}]\!]_F,\, \bar{u}_\mathcal{T}\big)_F - 2\big(f,\, \bar{u}_\mathcal{T}\big)\\ &= \Big\|A^{-1/2}(\boldsymbol{\sigma}_\mathcal{T}^\Delta + \boldsymbol{\sigma}_\mathcal{T}^c)\Big\|_0^2 + 2\sum_{K\in\mathcal{T}}\big(\nabla\cdot\boldsymbol{\sigma}_\mathcal{T},\, \bar{u}_\mathcal{T}\big)_K\\ &\quad + 2\sum_{F\in\mathcal{F}}\big([\![\boldsymbol{\sigma}_\mathcal{T}\cdot\boldsymbol{n}]\!]_F,\, \bar{u}_\mathcal{T}\big)_F - 2\big(f,\, \bar{u}_\mathcal{T}\big).\end{aligned}$$

By Lemma 3.1, $\big(\nabla\cdot\boldsymbol{\sigma}_\mathcal{T},\, \bar{u}_\mathcal{T}\big)$ cancels with $-\big(f,\, \bar{u}_\mathcal{T}\big)$, and the face integral term vanishes. Finally

$$\begin{aligned}\|u - \bar{u}_\mathcal{T}\|_A &\leq \Big(2\mathcal{J}(\bar{u}_\mathcal{T}) - 2\mathcal{J}^*(\boldsymbol{\sigma}_\mathcal{T})\Big)^{1/2}\\ &= \Big\|A^{-1/2}(\boldsymbol{\sigma}_\mathcal{T}^\Delta + \boldsymbol{\sigma}_\mathcal{T}^c)\Big\|_0 \leq \Big\|A^{-1/2}\boldsymbol{\sigma}_\mathcal{T}^\Delta\Big\|_0 + \Big\|A^{-1/2}\boldsymbol{\sigma}_\mathcal{T}^c\Big\|_0 .\end{aligned} \tag{3.27}$$

and

For the second term, by the estimate (3.19) for the second term, the following estimate holds

$$\|\boldsymbol{\sigma}_\mathcal{T}^c\|_{0,K} \leq C\, h_K \sum_{\boldsymbol{z}\in\mathcal{N}_K} \|c_{\boldsymbol{z}}\|_{0,K} ,$$

which is the sum of the violation of the Galerkin orthogonality for every interior vertex in K. By Lemma 3.4, and the shape regularity of the mesh, the following estimate holds:

$$\|\boldsymbol{\sigma}_{\mathcal{T}}^{c}\|_{0,K} \leq C \left\|A^{1/2}\right\|_{\infty,\omega_{\boldsymbol{z}}} \|u_{\mathcal{T}} - \bar{u}_{\mathcal{T}}\|_{A,\omega_K}.$$

As a result

$$\left\|A^{-1/2}\boldsymbol{\sigma}_{\mathcal{T}}^{c}\right\|_{0} = \left(\sum_{K\in\mathcal{T}} \left\|A^{-1/2}\boldsymbol{\sigma}_{\mathcal{T}}^{c}\right\|_{0,K}^{1/2}\right)^{1/2} \leq C_A \|u_{\mathcal{T}} - \bar{u}_{\mathcal{T}}\|_{A},$$

and the theorem follows follows from the definition of the global error estimator (3.21) for the first term in (3.27). □

The following lemma establishes the equivalence of the L^2-norm of any $\boldsymbol{\mathcal{RT}}^0_{-1,\omega_{\boldsymbol{z}}}$ function solving the local problem with the conventional residual-type local error indicator associated with a vertex. The unweighted version is Lemma 3 in [9], the weighted version is Theorem 5.11 in [16].

Lemma 3.6 ($\boldsymbol{H}$(div)-lifting estimate)**.** *If* $\left(g_K, 1\right)_{\mathcal{T}_{\boldsymbol{z}}} - \left(g_F, 1\right)_{\mathcal{F}_{\boldsymbol{z}}} = 0$*, then for the* $\boldsymbol{\sigma} \in \boldsymbol{\mathcal{RT}}^0_{-1,\omega_{\boldsymbol{z}}}$ *satisfying*

$$\begin{cases} \nabla\cdot\boldsymbol{\sigma} = g_K, & \text{on } K \subset \omega_{\boldsymbol{z}}, \\ [\![\boldsymbol{\sigma}\cdot\boldsymbol{n}]\!] = g_F, & \text{on } F \in \mathcal{F}_{\boldsymbol{z}}, \\ \boldsymbol{\sigma}\cdot\boldsymbol{n} = 0, & \text{on } F \subset \partial\omega_{\boldsymbol{z}}\backslash\partial\Omega, \end{cases} \tag{3.28}$$

with the minimal weighted L^2*-norm:* $\left\|A^{-1/2}(\cdot)\right\|_{0,\omega_{\boldsymbol{z}}}$*. Then the following a priori estimate holds with constant independent of the coefficient jumps under the Assumption 3.2:*

$$\left\|A^{-1/2}\boldsymbol{\sigma}\right\|_{0,\omega_{\boldsymbol{z}}} \leq C \left(\sum_{K\subset\omega_{\boldsymbol{z}}} h_K^2 A_K^{-1} \|g_K\|_{0,K}^2 + \sum_{F\in\mathcal{F}_{\boldsymbol{z}}} h_F A_F^{-1} \|g_F\|_{0,F}^2\right)^{1/2}. \tag{3.29}$$

Theorem 3.7 (Local efficiency bound for the total error indicator)**.**

$$C\eta_{D,\,\boldsymbol{z}} \leq \|u - \bar{u}_{\mathcal{T}}\|_{A,\omega_{\boldsymbol{z}}}, \tag{3.30}$$

where C *is independent of the coefficient distribution when Assumption 3.2 is met.*

Proof. To use Lemma 3.6, first we verify the local compatibility condition of the data: by (3.14) and (3.15)

$$\begin{aligned} &\left(\bar{r}_{K,\boldsymbol{z}} + \alpha_{K,\boldsymbol{z}} c_{\boldsymbol{z}},\, 1\right)_{\mathcal{T}_{\boldsymbol{z}}} - \left(\bar{j}_{F,\boldsymbol{z}},\, 1\right)_{\mathcal{F}_{\boldsymbol{z}}} \\ &= \left(\bar{r}_{K,\boldsymbol{z}},\, 1\right)_{\mathcal{T}_{\boldsymbol{z}}} - \left(\bar{j}_{F,\boldsymbol{z}},\, 1\right)_{\mathcal{F}_{\boldsymbol{z}}} + \sum_{K\subset\omega_{\boldsymbol{z}}^A} |K| \frac{1}{|\omega_{\boldsymbol{z}}^A|} \Big(\left(\bar{j}_{F,\boldsymbol{z}},\, 1\right)_{\mathcal{F}_{\boldsymbol{z}}} - \left(\bar{r}_{K,\boldsymbol{z}},\, 1\right)_{\mathcal{T}_{\boldsymbol{z}}}\Big) = 0. \end{aligned}$$

Rewriting the jump term in (3.12) as

$$[\![\boldsymbol{\sigma}^{\Delta}_{\boldsymbol{z},\mathcal{T}} \cdot \boldsymbol{n}_F]\!]_F = \bar{j}_{F,\boldsymbol{z}} = \Pi_F\Big(\phi_{\boldsymbol{z}}[\![(A\nabla(u-\bar{u}_{\mathcal{T}}))\cdot \boldsymbol{n}_F]\!]_F\Big),$$

then by Lemma 3.6, problem (3.12) has the following a priori estimate:

$$\begin{aligned} C\left\|A^{-1/2}\boldsymbol{\sigma}^{\Delta}_{\boldsymbol{z},\mathcal{T}}\right\|^2_{0,\omega_{\boldsymbol{z}}} \leq & \sum_{K\subset\omega_{\boldsymbol{z}}} h_K^2 A_K^{-1}\left\|\bar{r}_K\right\|^2_{0,K} + \sum_{K\subset\omega_{\boldsymbol{z}}} h_K^2 A_K^{-1}\left\|\alpha_{K,\boldsymbol{z}} c_{\boldsymbol{z}}\right\|^2_{0,K} \\ & + \sum_{F\in\mathcal{F}_{\boldsymbol{z}}} h_F A_F^{-1}\left\|[\![A\nabla(u-\bar{u}_{\mathcal{T}})\cdot\boldsymbol{n}_F]\!]_F\right\|^2_{0,F}, \end{aligned} \tag{3.31}$$

where for any $F = \overline{K^+}\cap\overline{K^-}$, $A_F := (A_{K^+}+A_{K^-})/2$.

Noted that the the standard bubble function trick works for any function in the finite element space (e.g. see the local efficiency proof in [33]), as a result the the element residual term and jump term have the following estimates:

$$\begin{aligned} C\, h_K A_K^{-1/2}\left\|\bar{r}_K\right\|_{0,K} &\leq \left\|u-\bar{u}_{\mathcal{T}}\right\|_{A,K}, \\ \text{and } C h_F^{1/2} A_F^{-1/2}\left\|[\![A\nabla(u-\bar{u}_{\mathcal{T}})\cdot\boldsymbol{n}_F]\!]_F\right\|_{0,F} &\leq \left\|u-\bar{u}_{\mathcal{T}}\right\|_{A,\omega_F}. \end{aligned} \tag{3.32}$$

Squaring and summing up both lead to:

$$\begin{aligned} C\sum_{K\subset\omega_{\boldsymbol{z}}} h_K^2 A_K^{-1}\left\|\bar{r}_K\right\|^2_{0,K} &\leq \left\|u-\bar{u}_{\mathcal{T}}\right\|^2_{A,\omega_{\boldsymbol{z}}}. \\ C\sum_{F\in\mathcal{F}_{\boldsymbol{z}}} h_F A_F^{-1}\left\|[\![A\nabla(u-\bar{u}_{\mathcal{T}})\cdot\boldsymbol{n}_F]\!]_F\right\|^2_{0,F} &\leq \left\|u-\bar{u}_{\mathcal{T}}\right\|^2_{A,\omega_{\boldsymbol{z}}}. \end{aligned} \tag{3.33}$$

For the algebraic error part $c_{\boldsymbol{z}}$ term in (3.31), by the first inequality in (3.23) from Lemma 3.4, the definition of the weight $\alpha_{K,\boldsymbol{z}}$ in (3.15), and the fact that the coefficient $A_K = \max\limits_{K'\subset\omega_{\boldsymbol{z}}} A_{K'}$ if $K\subset\omega^A_{\boldsymbol{z}}$, we have

$$\begin{aligned} &\sum_{K\subset\omega_{\boldsymbol{z}}} h_K^2 A_K^{-1}\left\|\alpha_{K,\boldsymbol{z}} c_{\boldsymbol{z}}\right\|^2_{0,K} = \sum_{K\subset\omega^A_{\boldsymbol{z}}} h_K^2 A_K^{-1}\frac{|\omega_{\boldsymbol{z}}|}{|\omega^A_{\boldsymbol{z}}|}\left\|c_{\boldsymbol{z}}\right\|^2_{0,K} \\ \leq & C\sum_{K\subset\omega^A_{\boldsymbol{z}}} A_K^{-1}\frac{|\omega_{\boldsymbol{z}}|}{|\omega^A_{\boldsymbol{z}}|}\big(\max_{K\subset\omega_{\boldsymbol{z}}} A_K\big)\left\|u-\bar{u}_{\mathcal{T}}\right\|^2_{A,\omega_{\boldsymbol{z}}} \\ \leq & C\left\|u-\bar{u}_{\mathcal{T}}\right\|^2_{A,\omega_{\boldsymbol{z}}}. \end{aligned} \tag{3.34}$$

Thus the local efficiency for the total error indicator $\eta_{D,\boldsymbol{z}}$ in (3.30) follows.

Lastly, when $\boldsymbol{z}\in\partial\Omega$ is the boundary vertex, applying the inequality (3.24) instead of (3.23) yields the same estimate. □

4 Algebraic error estimation and stopping criterion

The reliability bound (3.26) has the algebraic part of error $\|u_{\mathcal{T}} - \bar{u}_{\mathcal{T}}\|_A$ in it. In order that a stopping criterion can be inserted into any multigrid algorithm using this estimate, the algebraic error needs to be estimated. Recalling the stiffness matrix $\mathbf{A}$ introduced in Section 2, and the iterator matrix associated with 1 multigrid iteration is $\mathbf{B}$ from (2.7). Let the algebraic error at k-th iteration

$$\mathbf{e}^{(k)} := \mathbf{u}_{\mathcal{T}} - \mathbf{u}_{\mathcal{T}}^{(k)}, \tag{4.1}$$

then the error propagation can be verified to be:

$$\mathbf{e}^{(k+1)} = (\mathbf{I} - \mathbf{BA})\mathbf{e}^{(k)}. \tag{4.2}$$

Let $e^{(k)}$ be the function in the finite element space having $\mathbf{e}^{(k)}$ as its vector representation in the nodal basis. Define the spectral radius of the error propagation matrix $\mathbf{I} - \mathbf{BA}$ as ρ_{err}:

$$\rho_{\text{err}} := \rho(\mathbf{I} - \mathbf{BA}) = \|\mathbf{I} - \mathbf{BA}\|_2 . \tag{4.3}$$

Theorem 4.1 (Upper bound estimate of the algebraic error)**.** *If $\mathbf{e}^{(k)}$ is define in (4.1), $u_{\mathcal{T}}^{(k)}$ is the current iterate with $\mathbf{u}^{(k)}$ being its vector representation in the finite element nodal basis. The new iterate $u_{\mathcal{T}}^{(k)}$ and $\mathbf{u}^{(k)}$ are obtained by (2.7), then the following estimate holds:*

$$\left\|\mathbf{e}^{(k+1)}\right\|_{\mathbf{A}} \leq \frac{\rho_{\text{err}}}{1-\rho_{\text{err}}} \left\|\mathbf{u}^{(k+1)} - \mathbf{u}^{(k)}\right\|_{\mathbf{A}}, \tag{4.4}$$

or in the finite element function form:

$$\left\|u_{\mathcal{T}} - u_{\mathcal{T}}^{(k+1)}\right\|_A \leq \frac{\rho_{\text{err}}}{1-\rho_{\text{err}}} \left\|u_{\mathcal{T}}^{(k+1)} - u_{\mathcal{T}}^{(k)}\right\|_A . \tag{4.5}$$

Proof. Firstly we notice by the norm equivalence (2.10), the $\mathbf{A}$-norm of the error propagation matrix is

$$\|\mathbf{I} - \mathbf{BA}\|_{\mathbf{A}} = \left\|\mathbf{A}^{1/2}(\mathbf{I} - \mathbf{BA})\mathbf{A}^{-1/2}\right\|_2 = \rho\big(\mathbf{I} - \mathbf{A}^{1/2}\mathbf{B}\mathbf{A}^{1/2}\big). \tag{4.6}$$

Since $\mathbf{A}^{1/2}$ is non-singular, $\mathbf{A}^{1/2}(\mathbf{I} - \mathbf{BA})\mathbf{A}^{-1/2}$ and $\mathbf{I} - \mathbf{BA}$ are similar, and their spectrum radii coincide:

$$\left\|\mathbf{A}^{1/2}(\mathbf{I} - \mathbf{BA})\mathbf{A}^{-1/2}\right\|_2 = \|\mathbf{I} - \mathbf{BA}\|_2 = \rho\big(\mathbf{I} - \mathbf{BA}\big) = \rho_{\text{err}}. \tag{4.7}$$

Using the same reasoning, the following norm equivalence holds as well:

$$\|\mathbf{BA}\|_{\mathbf{A}} = \left\|\mathbf{A}^{1/2}(\mathbf{I} - \mathbf{BA})\mathbf{A}^{-1/2}\right\|_2 = \rho\big(\mathbf{BA}\big) = \lambda_{\max}(\mathbf{BA}). \tag{4.8}$$

By the error propagation formula (4.2),

$$\left\|\mathbf{e}^{(k+1)}\right\|_{\mathbf{A}} = \left\|(\mathbf{I} - \mathbf{BA})\mathbf{e}^{(k)}\right\|_{\mathbf{A}} \leq \|\mathbf{I} - \mathbf{BA}\|_{\mathbf{A}} \left\|\mathbf{e}^{(k)}\right\|_{\mathbf{A}} = \rho_{\text{err}} \left\|\mathbf{e}^{(k)}\right\|_{\mathbf{A}} . \tag{4.9}$$

Similarly, by the fact that the iterator $\mathbf{B}$ is non-singular, and $\lambda_{\min}(\mathbf{M}) = \big(\lambda_{\max}(\mathbf{M})\big)^{-1}$ given $\mathbf{M}$ is a non-singular matrix,

$$\begin{aligned} \left\|\mathbf{e}^{(k)}\right\|_{\mathbf{A}} &= \left\|(\mathbf{BA})^{-1}\mathbf{BAe}^{(k)}\right\|_{\mathbf{A}} \\ \leq \left\|(\mathbf{BA})^{-1}\right\|_{\mathbf{A}} \left\|\mathbf{BAe}^{(k)}\right\|_{\mathbf{A}} &\leq \frac{1}{\lambda_{\min}(\mathbf{BA})} \left\|\mathbf{BAe}^{(k)}\right\|_{\mathbf{A}}. \end{aligned} \tag{4.10}$$

To bridge (4.10) with (4.9) , first applying the triangle inequality in the definition (2.8):

$$\begin{aligned} \rho_{\text{err}} &= \sup_{\|\mathbf{v}\|_2=1} \|\mathbf{v} - \mathbf{BAv}\|_2 \geq \sup_{\|\mathbf{v}\|_2=1} \Big(\|\mathbf{v}\|_2 - \|\mathbf{BAv}\|_2 \Big) \\ &= \sup_{\|\mathbf{v}\|_2=1} \|\mathbf{v}\|_2 - \inf_{\|\mathbf{v}\|_2=1} \|\mathbf{BAv}\|_2 = 1 - \lambda_{\min}(\mathbf{BA}). \end{aligned} \tag{4.11}$$

For $\mathbf{BAe}^{(k)}$, combining (4.1) and (4.2) yields:

$$\mathbf{BAe}^{(k)} = \mathbf{e}^{(k)} - (\mathbf{I} - \mathbf{BA})\mathbf{e}^{(k)} = \mathbf{e}^{(k)} - \mathbf{e}^{(k+1)} = \mathbf{u}^{(k+1)} - \mathbf{u}^{(k)}. \tag{4.12}$$

Plugging (4.11) and (4.12) into (4.10) yields:

$$\left\|\mathbf{e}^{(k)}\right\|_{\mathbf{A}} \leq \frac{1}{1 - \rho_{\text{err}}} \left\|\mathbf{u}^{(k+1)} - \mathbf{u}^{(k)}\right\|_{\mathbf{A}}, \tag{4.13}$$

thus the final estimate (4.4) simply follows from (4.9). □

In Theorem 4.1, ρ_{err} is the true rate of convergence of the solver. However, in practice, the ρ_{err} is not accessible during any finite iteration of the solver, unless an eigenvalue problem is solved for the error propagation matrix $\mathbf{I} - \mathbf{BA}$. What we can have access is the following quantity:

$$\rho_{\text{err}}^{(k)} := \frac{\|\mathbf{r}_k\|_2}{\|\mathbf{r}_{k-1}\|_2}, \tag{4.14}$$

where $\mathbf{r}_k := \mathbf{Ae}^{(k)}$ with its j-th entry being $(f, \phi_{\boldsymbol{z}_j}) - \big(A\nabla u_{\mathcal{T}}^{(k)}, \nabla\phi_{\boldsymbol{z}_j}\big)$. The following lemma tells the convergence of $\rho_{\text{err}}^{(k)}$ provided that the iterative solver is convergent.

Lemma 4.2 (Convergence of $\rho_{\text{err}}^{(k)}$)**.** *Assuming the error propagation matrix* $\mathbf{I} - \mathbf{BA}$ *has eigenvalues* $1 > \rho_{\text{err}} = \lambda_1 \geq \lambda_2 \geq \cdots \geq \lambda_N > 0$*, then* $\rho_{\text{err}}^{(k)} \to \rho_{\text{err}}$ *as* $k \to \infty$*.*

Proof. First notice that, by applying (4.2) from 0 to k in a cascading fashion as well as $\mathbf{I} - \mathbf{BA}$ and $\mathbf{A}$ being symmetric,

$$\mathbf{r}_k = \mathbf{Ae}^{(k)} = \mathbf{A}(\mathbf{I} - \mathbf{BA})^k\mathbf{e}^{(0)} = (\mathbf{I} - \mathbf{AB})^k\mathbf{Ae}^{(0)} = (\mathbf{I} - \mathbf{AB})^k\mathbf{r}_0.$$

Since $\mathbf{A}(\mathbf{I} - \mathbf{AB})\mathbf{A}^{-1} = \mathbf{I} - \mathbf{BA}$, they share the same eigenpairs. Suppose that $\{\mathbf{v}_i\}_{i=1}^N$ be the set of orthonormal eigenvectors in ℓ^2-sense corresponding to the eigenvalue set

$\{\lambda_i\}_{i=1}^N$. Let $c_i = \mathbf{r}_0 \cdot \mathbf{v}_i$ be the coefficient of the eigen-expansion of the. Without loss of generality, assume the multiplicity of the largest eigenvalue λ_1 is 1. Then we have:

$$\begin{aligned}\rho_{\text{err}}^{(k)} &= \frac{\left\|(\mathbf{I}-\mathbf{AB})^{k+1}\mathbf{r}_0\right\|_2}{\|(\mathbf{I}-\mathbf{AB})^k\mathbf{r}_0\|_2} = \frac{\left\|\sum_{i=1}^N \lambda_i^{k+1} c_i \mathbf{v}_i\right\|_2}{\left\|\sum_{i=1}^N \lambda_i^k c_i \mathbf{v}_i\right\|_2} \\ &= \lambda_1 \frac{\left\|\sum_{i=1}^N \left(\frac{\lambda_i}{\lambda_1}\right)^{k+1} c_i \mathbf{v}_i\right\|_2}{\left\|\sum_{i=1}^N \left(\frac{\lambda_i}{\lambda_1}\right)^{k} c_i \mathbf{v}_i\right\|_2} = \lambda_1 \frac{1+\sum_{i=2}^N b_i \gamma_i^{k+1}}{1+\sum_{i=2}^N b_i \gamma_i^k},\end{aligned} \tag{4.15}$$

where $b_i := (c_i/c_1)^2$, and $\gamma_i := (\lambda_i/\lambda_1)^2$. The lemma follows from letting $k \to \infty$. When the multiplicity of λ_1 is $m \geq 2$, factoring out the first m terms and i starts from $(m+1)$ in the eigen-expansion in (4.15) yields the same result.

□

Lemma 4.3 (Monotonicity of $\rho_{\text{err}}^{(k)}$)**.** *Under the same assumption as in Lemma 4.2,* $\rho_{\text{err}}^{(k-1)} \leq \rho_{\text{err}}^{(k)}$*, for any* $k \in \mathbb{Z}^+$*.*

Proof. To prove this lemma, it suffices to show that:

$$\begin{aligned}&\left(1+\sum_{i=2}^N b_i\gamma_i^k\right)^2 \leq \left(1+\sum_{i=2}^N b_i\gamma_i^{k-1}\right)\left(1+\sum_{i=2}^N b_i\gamma_i^{k+1}\right) \\ \iff\quad & 1+2\sum_{i=2}^N b_i\gamma_i^k + \left(\sum_{i=2}^N b_i\gamma_i^k\right)^2 \\ \leq\ & 1+\sum_{i=2}^N b_i\left(\gamma_i^{k-1}+\gamma_i^{k-1}\right) + \left(\sum_{i=2}^N b_i\gamma_i^{k-1}\right)\left(\sum_{i=2}^N b_i\gamma_i^{k+1}\right).\end{aligned} \tag{4.16}$$

The inequality between the second terms in both left and right hand sides can be proved as follows:

$$2\gamma_i^k \leq \gamma_i^{k-1}+\gamma_i^{k+1} \iff 0 \leq (1-\gamma_i)^2.$$

Then it suffices to show that the following inequality is true:

$$\left(\sum_{i=2}^N b_i\gamma_i^k\right)^2 \leq \left(\sum_{i=2}^N b_i\gamma_i^{k-1}\right)\left(\sum_{i=2}^N b_i\gamma_i^{k+1}\right). \tag{4.17}$$

A standard inductive argument is as follows: when $N=2$, the equality in (4.17) holds. Now we assume that (4.17) holds for $N=n$. When $N=n+1$: we can bound

the left hand side of (4.17) by induction hypothesis

$$\begin{aligned}&\left(\sum_{i=2}^{n} b_i\gamma_i^k + b_{n+1}\gamma_{n+1}^k\right)^2\\ &\leq \left(\sum_{i=2}^{n} b_i\gamma_i^{k-1}\right)\left(\sum_{i=2}^{n} b_i\gamma_i^{k+1}\right) + \left(b_{n+1}\gamma_{n+1}^k\right)^2 + 2b_{n+1}\gamma_{n+1}^k\sum_{i=2}^{n} b_i\gamma_i^k.\end{aligned} \tag{4.18}$$

And the right hand side of (4.17) equals

$$\begin{aligned}&\left(\sum_{i=2}^{n} b_i\gamma_i^{k-1}\right)\left(\sum_{i=2}^{n} b_i\gamma_i^{k+1}\right) + b_{n+1}^2\gamma_{n+1}^{k-1}\gamma_{n+1}^{k+1}\\ &+b_{n+1}\gamma_{n+1}^{k+1}\left(\sum_{i=2}^{n} b_i\gamma_i^{k-1}\right) + b_{n+1}\gamma_{n+1}^{k-1}\left(\sum_{i=2}^{n} b_i\gamma_i^{k+1}\right).\end{aligned} \tag{4.19}$$

Now it suffices to show that:

$$2b_{n+1}\gamma_{n+1}^k\sum_{i=2}^{n} b_i\gamma_i^k \leq b_{n+1}\gamma_{n+1}^{k+1}\left(\sum_{i=2}^{n} b_i\gamma_i^{k-1}\right) + b_{n+1}\gamma_{n+1}^{k-1}\left(\sum_{i=2}^{n} b_i\gamma_i^{k+1}\right)$$

This is equivalent to show that for each term $i = 2, \cdots, n$

$$2\gamma_{n+1}^k\gamma_i^k \leq \gamma_{n+1}^{k+1}\gamma_i^{k-1} + \gamma_{n+1}^{k-1}\gamma_i^{k+1} \Longleftrightarrow 2\gamma_{n+1}\gamma_i \leq \gamma_{n+1}^2 + \gamma_i^2 \Longleftrightarrow 0 \leq (\gamma_i - \gamma_{n+1})^2.$$

Thus the lemma. □

After the preparation, now we define the algebraic error estimator as follows at the $(k+1)$-th iteration of the solver: for $k \geq 1$

$$\eta_A^{(k+1)} := e^{1/k}\frac{\rho_{\text{err}}^{(k)}}{1-\rho_{\text{err}}^{(k)}}\left\|\mathbf{u}^{(k+1)} - \mathbf{u}^{(k)}\right\|_{\mathbf{A}} = e^{1/k}\frac{\rho_{\text{err}}^{(k)}}{1-\rho_{\text{err}}^{(k)}}\left\|u_{\mathcal{T}}^{(k+1)} - u_{\mathcal{T}}^{(k)}\right\|_A. \tag{4.20}$$

The $e^{1/k}$ factor is added artificially to remedy the fact that $\rho_{\text{err}}^{(k)}$ converges to ρ_{err} from below. Moreover, this factor makes up for the first few iterations, in which the fast converging of the solver results $\rho_{\text{err}}^{(k)}$ small.

Theorem 4.4 (Reliability of the algebraic error estimator)**.** *Under the same setting with Theorem 4.1 and Lemma 4.2, there exists an $N \in \mathbb{Z}^+$ such that for all $k \geq N$,*

$$\left\|\mathbf{e}^{(k+1)}\right\|_{\mathbf{A}} = \left\|u_{\mathcal{T}} - u_{\mathcal{T}}^{(k+1)}\right\|_A \leq \eta_A^{(k+1)}. \tag{4.21}$$

Proof. Denote $p(k) := \rho_{\text{err}}^{(k)}$, $\xi(k) := p(k)/\Big(1-p(k)\Big)$, and $\xi(\infty) := \rho_{\text{err}}/(1-\rho_{\text{err}})$. By Theorem 4.1, it suffices to show that: there exists an N such that for $k \geq N$

$$\xi(\infty) \leq e^{1/k}\xi(k). \tag{4.22}$$

It is straightforward to verify that $\xi(k) \to \xi(\infty)$ from below as $p(k) \to \rho_{\text{err}}$. Moreover, $e^{1/k}\xi(k) \to \xi(\infty)$ as $k \to \infty$. Now it suffices to show that when k is sufficiently large, $e^{1/k}\xi(k)$ is a decreasing function of k. Recalling from (4.15) in Lemma 4.2 that when $k \to \infty$,

$$p(k) \simeq \rho_{\text{err}} \frac{1 + b\gamma^{k+1}}{1 + b\gamma^k}, \tag{4.23}$$

where $\gamma := (\lambda_{m+1}/\lambda_1)^2 < 1$, and $b := (c_{m+1}/c_1)^2 \geq 0$ if m is the multiplicity of the largest eigenvalue. Taking derivative of $e^{1/k}\xi(k)$ with respect to k leads to:

$$\begin{aligned} \frac{d}{dk}\big(e^{1/k}\xi(k)\big) &= e^{1/k}\left(-\frac{1}{k^2}\right)\xi(k) + e^{1/k}\xi'(k) \\ &= e^{1/k}\frac{-k^{-2}p(k)\big(1-p(k)\big) + p'(k)}{\big(1-p(k)\big)^2}. \end{aligned} \tag{4.24}$$

By (4.23), we have

$$p'(k) \simeq \rho_{\text{err}} \frac{b(\gamma-1)\gamma^k \ln \gamma}{\big(1 + b\gamma^k\big)^2} = O(\gamma^k). \tag{4.25}$$

Lastly, using above as $p'(k)$'s order in (4.24), and $p(k)\big(1-p(k)\big) \to \rho_{\text{err}}(1-\rho_{\text{err}})$, since $p'(k) \simeq O(\gamma^k) = o(k^{-2})$ as $k \to \infty$, $\frac{d}{dk}(e^{1/k}\xi(k)) < 0$ for sufficiently large k, and the theorem follows. □

Now the inexact AFEM cycle with a guaranteed stopping criterion is presented in Algorithm 1. The stopping criterion is designed with Theorem 3.5, Theorem 4.4, and identity (1.2) in mind. Generally speaking, the iterative solver stops when the algebraic error estimator η_A drops below certain tolerance ratio of the total error estimator η_D. This indicates that the estimated algebraic error drops below certain percentage of the total error. Moreover, in order that η_A is an accurate representation of the algebraic error $\left\|u_{\mathcal{T}} - u_{\mathcal{T}}^{(k)}\right\|_A$ at k-th iteration, in light of the proof of Theorem 4.4, $\rho_{\text{err}}^{(k)}$ needs to be an accurate representation of ρ_{err} as well.

Remark 4.5 (Speed up of the rate of convergence estimate). We notice that without the correction factor in (4.20), the closer $\rho_{\text{err}}^{(k)}$ is to ρ_{err}, the more accurate the algebraic estimator is. The convergence of $\rho_{\text{err}}^{(k)}$ can be accelerated in the following way:

$$\rho_{\text{err}}^{(k)} \approx \rho_{\text{err}} \frac{1 + b\gamma^{k+1}}{1 + b\gamma^k} \quad \text{, and} \quad \rho_{\text{err}}^{(k-1)} \approx \rho_{\text{err}} \frac{1 + b\gamma^{k}}{1 + b\gamma^{k-1}}.$$

Now we define for $k \geq 2$:

$$\widehat{\rho}_{\text{err}}^{(k)} := \rho_{\text{err}}^{(k)} \frac{\rho_{\text{err}}^{(k)}}{\rho_{\text{err}}^{(k-1)}}. \tag{4.26}$$

And $\widehat{\rho}_{\text{err}}^{(k)} \to \rho_{\text{err}}$ faster than the original $\rho_{\text{err}}^{(k)}$. To see this, taking derivative of $\widehat{\rho}_{\text{err}}^{(k)}$ with respect to k gives,

$$\frac{d}{dk}\big(\widehat{\rho}_{\text{err}}^{(k)}\big) = O(\gamma^{k-1}),$$

Algorithm 1 Inexact adaptive finite element (AFEM) cycle and stopping criterion

Input: Current data structures based on $\mathcal{T}^{(m)}$, initial guess $\mathbf{u}^{(0)}$, tolerance for estimator $\texttt{tol}$, tolerance for $\rho_{\mathrm{err}}^{(k)}$ $\texttt{tol}_\rho$.

Output: Adaptively refined mesh $\mathcal{T}^{(m+1)}$, iterate $\mathbf{u}^{(k+1)}$ on $\mathcal{T}^{(m)}$.

procedure ITERATE $\longrightarrow$ ESTIMATE $\longrightarrow$ MARK $\longrightarrow$ REFINE

ITERATE:
  Initial guess $\leftarrow \mathbf{u}^{(0)}$ on $\mathcal{T}^{(m)}$.
  Perform k iterations of the solver for (2.6) to get $\mathbf{u}^{(k)}$.
ESTIMATE:
  Compute $\eta_D^{(k)}$ and $\eta_{D,K}^{(k)}$ in (3.21) using $\mathbf{u}^{(k)}$.
  Compute $\rho_{\mathrm{err}}^{(k)}$, $\rho_{\mathrm{err}}^{(k-1)}$, and $\eta_A^{(k)}$ in (4.20) using $\mathbf{u}^{(k)}$ and $\mathbf{u}^{(k-1)}$.
  if $\eta_A^{(k)} > (\texttt{tol}) \cdot \eta_D^{(k)}$ **or** $\left|\rho_{\mathrm{err}}^{(k)}/\rho_{\mathrm{err}}^{(k-1)} - 1\right| > \texttt{tol}_\rho$ **then** ▷ Continue.
    $\mathbf{u}^{(0)} \leftarrow \mathbf{u}^{(k)}$.
    goto ITERATE.
  else ▷ Stop.
    break;
MARK:
  Mark the elements using $\eta_{D,K}^{(k)}$.
REFINE:
  Refine the marked elements to get $\mathcal{T}^{(m+1)}$.
  $m \leftarrow m+1$.
  goto ITERATE.

which is an order faster than the convergence of $\rho_{\mathrm{err}}^{(k)}$ in (4.25).

5 Explicit construction of the local problems

This section covers the explicit construction of the local problem in Section 3.2 in a linear solver package oriented form. It is assumed that the user has access to the data structures for the original problem, as well as certain extra information like the AMS solver ([28]) in *hypre* ([26]).

It is known that the problem (3.12) with the minimization procedure is equivalent to the following hybridized-mixed problem on the patch (see [16]): Find $(\boldsymbol{\sigma}_{\boldsymbol{z},\mathcal{T}}^{\Delta}, e_{\boldsymbol{z},\mathcal{T}}, \lambda_{\boldsymbol{z},\mathcal{T}}) \in \boldsymbol{\mathcal{RT}}^0_{-1,\omega_{\boldsymbol{z}}} \times \mathcal{S}_{\omega_{\boldsymbol{z}}} \times \mathcal{M}_{\omega_{\boldsymbol{z}}}$ such that

$$\begin{cases} \left(A^{-1}\boldsymbol{\sigma}_{\boldsymbol{z},\mathcal{T}}^{\Delta}, \boldsymbol{\tau}\right)_{\mathcal{T}_{\boldsymbol{z}}} - \left(e_{\boldsymbol{z},\mathcal{T}}, \nabla\cdot\boldsymbol{\tau}\right)_{\mathcal{T}_{\boldsymbol{z}}} + \left(\llbracket\boldsymbol{\tau}\cdot\boldsymbol{n}\rrbracket, \lambda_{\boldsymbol{z},\mathcal{T}}\right)_{\mathcal{F}_{\boldsymbol{z}}} = 0, \\ \left(\nabla\cdot\boldsymbol{\sigma}_{\boldsymbol{z},\mathcal{T}}^{\Delta}, w\right)_{\mathcal{T}_{\boldsymbol{z}}} = \left(\bar{r}_{K,\boldsymbol{z}}, w\right)_{\mathcal{T}_{\boldsymbol{z}}}, \\ \left(\llbracket\boldsymbol{\sigma}_{\boldsymbol{z},\mathcal{T}}^{\Delta}\cdot\boldsymbol{n}\rrbracket, \mu\right)_{\mathcal{F}_{\boldsymbol{z}}} = \left(\bar{j}_{F,\boldsymbol{z}}, \mu\right)_{\mathcal{F}_{\boldsymbol{z}}}, \end{cases} \tag{5.1}$$

for all $(\boldsymbol{\tau}, w, \mu) \in \boldsymbol{\mathcal{RT}}^0_{-1,\omega_{\boldsymbol{z}}} \times \mathcal{S}_{\omega_{\boldsymbol{z}}} \times \mathcal{M}_{\omega_{\boldsymbol{z}}}$, where $\boldsymbol{\mathcal{RT}}^0_{-1,\omega_{\boldsymbol{z}}}$ is the broken Raviart-Thomas space in (3.11), while $\mathcal{S}_{\omega_{\boldsymbol{z}}}$ and $\mathcal{M}_{\omega_{\boldsymbol{z}}}$ are the spaces of the piecewise constant defined in the element and the interior/Dirichlet edges in the patch $\omega_{\boldsymbol{z}}$:

$$\begin{aligned} \mathcal{S}_{\omega_{\boldsymbol{z}}} &:= \{w \in L^2(\omega_{\boldsymbol{z}}) : w\big|_K \in P^0(K),\ \forall K \subset \omega_{\boldsymbol{z}}\}, \\ \text{and}\ \ \mathcal{M}_{\omega_{\boldsymbol{z}}} &:= \{\mu \in L^2(\mathcal{F}_{\boldsymbol{z}}) : \mu\big|_F \in P^0(F),\ \forall F \in \mathcal{F}_{\boldsymbol{z}}\}. \end{aligned} \tag{5.2}$$

5.1 Equilibrated flux construction in 2D

In this subsection, we walk through how to perform the localized a posteriori error estimation based merely on minimally given data structures in a widely used setting in the actual practice of *hypre*. A concrete example on an unstructured local vertex patch is given together with formulas for the localized a posteriori error estimation. Similar data structure recovery techniques can be found in the MATLAB package *i*FEM document [18].

It is assumed that the user has the following quantities provided by solver (e.g. see *hypre* user manual Chapter 6):

- The stiffness matrix $\mathbf{A}$.
- The right hand side $\mathbf{f}$.
- The current iterate $\mathbf{u}$.
- The discrete gradient matrix $\mathbf{G} \in \{+1, -1, 0\}^{\dim \mathcal{F} \times \dim \mathcal{N}}$. $\mathbf{G}$ is encoded with the topology of the mesh structure. The i-th row corresponds to the i-th edge in the mesh. In i-th row, there are two nonzero entries: $+1$ and -1 in the columns corresponding to the vertices composing the i-th edge. The sign is determined based on the orientation of the edge. $\mathbf{G}$ includes all (interior and boundary) edges and vertices.
- The coordinates set $\{\boldsymbol{z}_i\}$ of all the vertices in the mesh.

The necessary data needed to solve the localized problem (5.1) in a semi-explicit procedure are listed as follows:

- $\bar{A}$: the approximated diffusion coefficient.
- $\mathbf{r}$: the approximated residual estimator vector representing element residual and edge jump.
- $\mathbf{M}$: the local mass matrix for the Raviart-Thomas elements associated with only the interior edges.

Throughout the rest of this subsection, we use the interior vertex patch consisting totally 7 vertices in Figure 1 as examples to illustrate how to construct these quantities. It is assumed that locally in the patch, the vertex $\boldsymbol{z}$ is labeled as $\boldsymbol{z}_1$. The rest of the

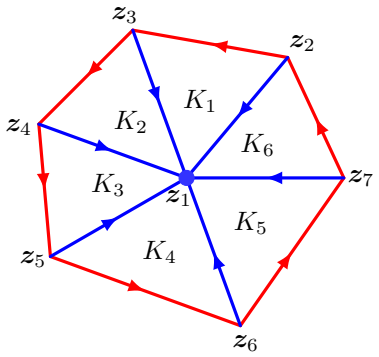

Figure 1: A vertex patch with interior edges marked in blue.

vertices are locally labeled counter-clockwisely in an ascending fashion with respect to $\boldsymbol{z}_1$. Following the fixed directions of edges shown in Figure 1, the local discrete gradient matrix block $\mathbf{G}_{\omega_{\boldsymbol{z}}}$ covering interior edges is as follows:

$$\mathbf{G}_{\omega_{\boldsymbol{z}}} = \begin{pmatrix} 1 & -1 & 0 & 0 & 0 & 0 & 0 \\ 1 & 0 & -1 & 0 & 0 & 0 & 0 \\ 1 & 0 & 0 & -1 & 0 & 0 & 0 \\ 1 & 0 & 0 & 0 & -1 & 0 & 0 \\ 1 & 0 & 0 & 0 & 0 & -1 & 0 \\ 1 & 0 & 0 & 0 & 0 & 0 & -1 \end{pmatrix}, \tag{5.3}$$

where the i-th row corresponds to the interior edge F_i joining vertices $\boldsymbol{z}_1$ and $\boldsymbol{z}_{i+1}$ $(i = 1, \ldots, 6)$. The local discrete gradient matrix block $\mathbf{G}_{\partial\omega_{\boldsymbol{z}}}$ covering boundary edges on $\partial\omega_{\boldsymbol{z}}$ is as follows:

$$\mathbf{G}_{\partial\omega_{\boldsymbol{z}}} = \begin{pmatrix} 0 & -1 & 1 & 0 & 0 & 0 & 0 \\ 0 & 0 & -1 & 1 & 0 & 0 & 0 \\ 0 & 0 & 0 & -1 & 1 & 0 & 0 \\ 0 & 0 & 0 & 0 & -1 & 1 & 0 \\ 0 & 0 & 0 & 0 & 0 & -1 & 1 \\ 0 & 1 & 0 & 0 & 0 & 0 & -1 \end{pmatrix}, \tag{5.4}$$

where the i-th row corresponds to the boundary edge F_{i+6} joining vertices $\boldsymbol{z}_{i+1}$ and $\boldsymbol{z}_{i+2}$ $(i = 1, \ldots, 6$, with $\boldsymbol{z}_8 = \boldsymbol{z}_2)$. The discrete gradient matrix block for this vertex patch is then $\mathbf{G}_{\boldsymbol{z}} = \begin{pmatrix} \mathbf{G}_{\omega_{\boldsymbol{z}}} \\ \mathbf{G}_{\partial\omega_{\boldsymbol{z}}} \end{pmatrix}$. The cardinality of nonzero entries in the first column of $\mathbf{G}_{\boldsymbol{z}}$ (corresponding the all the edges connected to $\boldsymbol{z}_1$) is equal to the number of the interior edges, and the number of elements in this vertex patch $|\mathcal{T}_{\boldsymbol{z}}|$ as well. For any vertex $\boldsymbol{z}$ having a global index $j_{\boldsymbol{z}}$, define

$$N_{\boldsymbol{z}} := \#\big\{i : \mathbf{G}[i, j_{\boldsymbol{z}}] = \mathbf{G}_{\boldsymbol{z}}[i, 1] \neq 0\big\}.$$

$N_{\boldsymbol{z}}$ for every vertex $\boldsymbol{z}$ can be obtained by counting the number of nonzero entries on the $j_{\boldsymbol{z}}$-th column of the global discrete gradient matrix $\mathbf{G}$.

To build the error estimator, the first step is to get element matrix from the discrete gradient matrix. The $\mathbf{G}_{\boldsymbol{z}}$ the consists all the necessary topological structure of the local elements. Let $\mathbf{T}_{\boldsymbol{z}} \in \mathbb{I}^{N_{\boldsymbol{z}} \times 3}$ be the element index matrix of $\omega_{\boldsymbol{z}}$, where $\mathbb{I} = \{1, \ldots, 7\}$ is the index set of all the vertices in $\omega_{\boldsymbol{z}}$. Then $\mathbf{T}_{\boldsymbol{z}}$ can be recovered using Algorithm 2. The i-th row $\mathbf{T}_{\boldsymbol{z}}[i, *]$ collects the indices of all vertices in the i-th element of this patch.

Algorithm 2 Assembling of the local element matrix

Input: $N_{\boldsymbol{z}}$, $\mathbf{G}_{\boldsymbol{z}}$
Output: $\mathbf{T}_{\boldsymbol{z}}$

for $i = 1$ to N_z **do** ▷ i follows the index of interior edges.
  $\mathbf{T}_{\boldsymbol{z}}[i, 1] \leftarrow 1$ ▷ The 1st vertex in each element is $\boldsymbol{z}_1$.
  for $j = 2$ to $N_z + 1$ **do** ▷ j follows the index of vertices.
    if $\mathbf{G}_{\boldsymbol{z}}[i, j] \neq 0$ **then**
      $\mathbf{T}_{\boldsymbol{z}}[i, 2] \leftarrow j$. ▷ Edge F_i joins $\boldsymbol{z}_1$ and the 2nd vertex.
      for $i_1 > i$, $j_1 \neq \mathbf{T}_{\boldsymbol{z}}[i-1, 2]$ **do** ▷ 0 index is empty.
        if $\mathbf{G}_{\boldsymbol{z}}[i_1, j] \neq 0$, $\mathbf{G}_{\boldsymbol{z}}[i_1, j_1] \neq 0$ **then**
          $\mathbf{T}_{\boldsymbol{z}}[i, 3] \leftarrow j_1$ ▷ Edge F_{i_1} joins $\boldsymbol{z}_j$ and the 3rd vertex.

Following Algorithm 2, the $\mathbf{T}_{\boldsymbol{z}}$ we obtain is

$$\mathbf{T}_{\boldsymbol{z}} = \begin{pmatrix} 1 & 2 & 3 \\ 1 & 3 & 4 \\ 1 & 4 & 5 \\ 1 & 5 & 6 \\ 1 & 6 & 7 \\ 1 & 7 & 2 \end{pmatrix}. \tag{5.5}$$

Notice that, following Algorithm 2, the neighboring elements for i-th interior edge (corresponding to the i-th row of $\mathbf{G}_{\boldsymbol{z}}$) are K_i and $K_{((i-2) \bmod N_{\boldsymbol{z}})+1}$, e.g., the 1st edge has element K_1 and element K_6 as its neighbors (corresponding to the 1-st row and the 6-th row in $\mathbf{T}_{\boldsymbol{z}}$).

For the i-th edge in the patch, without loss of generality, suppose the two nonzero entries on the i-th row of $\mathbf{G}_{\boldsymbol{z}}$ be $\mathbf{G}_{\boldsymbol{z}}[i, j_1] = 1$ and $\mathbf{G}_{\boldsymbol{z}}[i, j_2] = -1$, then the scaled tangential vector $\boldsymbol{t}_i$ of the i-th edge is then computed by: $\boldsymbol{t}_i = \boldsymbol{z}_{j_1} - \boldsymbol{z}_{j_2}$. The scaled norm vector is then $\boldsymbol{t}_i^{\perp}$.

Let $\mathbf{A}_{\boldsymbol{z}}$ be the local stiffness matrix block following the index setting in Figure 1, such that $\mathbf{A}_{\boldsymbol{z}}[i, j] = \left(A\nabla\phi_{\boldsymbol{z}_i}, \nabla\phi_{\boldsymbol{z}_j}\right)_{\omega_{\boldsymbol{z}}}$, and $\mathbf{f}_{\boldsymbol{z}}$ be the local right hand side block $\mathbf{f}_{\boldsymbol{z}}[j] = \left(f, \phi_{\boldsymbol{z}_j}\right)_{\omega_{\boldsymbol{z}}}$. Given the current iterate from the solver, $\mathbf{u}_{\boldsymbol{z}}$ is the the local solution with $\mathbf{u}_{\boldsymbol{z}}[j]$ being the coefficient of $\phi_{\boldsymbol{z}_j}$. Assuming the local vertex coordinates for $\boldsymbol{z}_i$ are stored in $\mathbf{x}_{\boldsymbol{z}}[i, *]$.

After retrieving the local element topological structure information, the next step is to assemble the local residual vector $\mathbf{r}_{\boldsymbol{z}}$, which consists the element residuals and edge jumps in (3.13). $\mathbf{r}_{\boldsymbol{z}}[2i-1]$ stores the approximated and scaled element residual on the local element K_i, and $\mathbf{r}_{\boldsymbol{z}}[2i]$ stores the approximated and scaled normal derivative

jump across the local edge F_i:

$$\mathbf{r}_{\boldsymbol{z}}[2i-1] \approx \bar{r}_{K_i,\boldsymbol{z}}|K_i| = \left(\bar{r}_{K_i,\boldsymbol{z}},\, 1_{K_i}\right)_{\mathcal{T}_{\boldsymbol{z}}},$$
$$\mathbf{r}_{\boldsymbol{z}}[2i] \approx \bar{j}_{F_i,\boldsymbol{z}}|F_i| = \left(\bar{j}_{F_i,\boldsymbol{z}},\, 1_{F_i}\right)_{\mathcal{F}_{\boldsymbol{z}}}.$$

The 1_{K_i} and 1_{F_i} are the indicator functions of element K_i, and edge F_i respectively, which are the bases for the test function spaces (5.2). In this setting, the vector $\mathbf{r}_{\boldsymbol{z}}$ stores the right hand sides of equation (5.1). Algorithm 3 performs the procedure to obtain $\mathbf{r}_{\boldsymbol{z}}$.

Algorithm 3 Assembling of the approximated local residual vector $\mathbf{r}_{\boldsymbol{z}}$

Input: $\mathbf{x}_{\boldsymbol{z}}$, $N_{\boldsymbol{z}_i}$ $(1 \le i \le N_{\boldsymbol{z}}+1)$, $\mathbf{G}_{\boldsymbol{z}}$, $\mathbf{T}_{\boldsymbol{z}}$, $\mathbf{A}_{\boldsymbol{z}}$, $\mathbf{f}_{\boldsymbol{z}}$, $\mathbf{u}_{\boldsymbol{z}}$.
Output: $\mathbf{r}_{\boldsymbol{z}}$

for $i = 1$ to N_z **do** ▷ i follows the indices of elements.
  $l_1 \leftarrow \mathbf{T}_{\boldsymbol{z}}[i,1], l_2 \leftarrow \mathbf{T}_{\boldsymbol{z}}[i,2], l_3 \leftarrow \mathbf{T}_{\boldsymbol{z}}[i,3]$.
  $k \leftarrow \left|\det \begin{pmatrix} \mathbf{x}_{\boldsymbol{z}}[l_3,*] - \mathbf{x}_{\boldsymbol{z}}[l_1,*] \\ \mathbf{x}_{\boldsymbol{z}}[l_2,*] - \mathbf{x}_{\boldsymbol{z}}[l_3,*] \end{pmatrix}\right|$. ▷ Twice the Area of K_i.
  for $j = 1$ to 3 **do** ▷ 3 vertices in an element.
    $l \leftarrow \mathbf{T}_{\boldsymbol{z}}[i,j]$
    $\mathbf{r}_{\boldsymbol{z}}[2i-1] \leftarrow \mathbf{r}_{\boldsymbol{z}}[2i-1] + \frac{1}{3N_{\boldsymbol{z}_l}}\mathbf{f}_{\boldsymbol{z}}[l]$.
    $\bar{A} \leftarrow \frac{1}{N_{\boldsymbol{z}_l}}\mathbf{A}_{\boldsymbol{z}}[l,l]$. ▷ The approximated diffusion coeffient.
    $l_1 \leftarrow \mathbf{T}_{\boldsymbol{z}}[i,(j-2) \mod 3+1]$, $l_2 \leftarrow \mathbf{T}_{\boldsymbol{z}}[i,j \mod 3+1]$.
    $\mathbf{n} \leftarrow (\mathbf{x}[l_1,*] - \mathbf{x}[l_2,*])^{\perp}$. ▷ The scaled inner normal vector opposite to local vertex j.
    $\mathbf{F}[i,*] \leftarrow \mathbf{F}[i,*] + \bar{A}\mathbf{u}_{\boldsymbol{z}}[l]\,\mathbf{n}/k$. ▷ The scaled numerical flux on each element.
for $i = 1$ to N_z **do** ▷ i follows the indices of interior edges.
  $i_1 \leftarrow i$, $i_2 \leftarrow (i-2) \bmod N_{\boldsymbol{z}} + 1$. ▷ The neighbor elements of edge i.
  if $\mathbf{G}_{\boldsymbol{z}}[i,l_1] = 1$, $\mathbf{G}_{\boldsymbol{z}}[i,l_2] = -1$, **then**
    $\mathbf{n} \leftarrow (\mathbf{x}[l_1,*] - \mathbf{x}[l_2,*])^{\perp}$.
  $\mathbf{r}_{\boldsymbol{z}}[2i] \leftarrow (\mathbf{F}[i_2,*] - \mathbf{F}[i_1,*])^T\,\mathbf{n}$.

Following the semi-explicit construction for problem (5.1) in [16], the discrete divergence with jump part of equations (5.1) can be constructed explicitly, i.e., a discontinuous flux correction in $\boldsymbol{\mathcal{RT}}^0_{-1,\omega_{\boldsymbol{z}}}$ can be recovered satisfying the second and the third equations exactly. Then a minimization procedure is carried over the kernel of the discrete divergence, so that a correction term in $\boldsymbol{\mathcal{RT}}^0_{\omega_{\boldsymbol{z}}}$ with continuous normal component is added to the flux correction term.

Locally in each element $K \subset \omega_{\boldsymbol{z}}$, the three basis functions of $\boldsymbol{\mathcal{RT}}^0(K)$ associated with three edges are defined as follows. For a K that corresponds to a row of $\mathbf{T}_{\boldsymbol{z}}$, the j-th edge is opposite to the j-th vertex (corresponding to the j-th column, $1 \le j \le 3$). Let $j_1 = (j-2) \mod 3+1$ be the vertex index opposite to the previous edge to j-th edge in the counterclockwise numbering setting, and $j_2 = j \mod 3+1$ be the vertex index opposite to the next edge to j-th edge. The basis function associated with this

j-th edge is then:

$$\boldsymbol{\psi}_j = \phi_{\boldsymbol{z}_{j_2}} \nabla^\perp \phi_{\boldsymbol{z}_{j_1}} - \phi_{\boldsymbol{z}_{j_1}} \nabla^\perp \phi_{\boldsymbol{z}_{j_2}}. \tag{5.6}$$

For the $\boldsymbol{\mathcal{RT}}^0_{-1,\omega_{\boldsymbol{z}}}$ space, a basis function of $\boldsymbol{\mathcal{RT}}^0(K)$ has support being K, with no neighboring elements involved. It can be verified that

$$\big(\nabla\cdot\boldsymbol{\psi}_j,\, 1_K\big)_{\mathcal{T}_{\boldsymbol{z}}} = 1, \text{ and } \big([\![\boldsymbol{\psi}_j \cdot \boldsymbol{n}]\!],\, 1_F\big)_{\mathcal{F}_{\boldsymbol{z}}} = 1, \tag{5.7}$$

where $F \subset \partial K$, if the edges always counterclockwisely oriented within K.

Let $\mathbf{s}_{\boldsymbol{z}}$ stores the coefficient array of the $\boldsymbol{\mathcal{RT}}^0_{-1,\omega_{\boldsymbol{z}}}$-basis functions associated with the interior edges on patch $\omega_{\boldsymbol{z}}$. Using the index from Figure 1, for any $1 \le i \le N_{\boldsymbol{z}}$, there are two coefficients associated with the basis of edge F_i: one within element K_i, stored in $\mathbf{s}[2i-1]$ and the other within element $K_{i'}$ with $i' = (i-2) \bmod N_{\boldsymbol{z}} + 1$, stored in $\mathbf{s}[2i']$. Let $\mathbf{D}_{\boldsymbol{z}} \in \mathbb{R}^{2N_{\boldsymbol{z}} \times 2N_{\boldsymbol{z}}}$ be the matrix associated with the discrete divergence with jump part of (5.1), where $\mathbf{D}_{\boldsymbol{z}}[2i-1, *]$ represent the divergence equation on i-th element, and $\mathbf{D}_{\boldsymbol{z}}[2i', *]$ represent the edge jump equation on i-th interior edge:

$$\mathbf{D}_{\boldsymbol{z}}\, \mathbf{s}_{\boldsymbol{z}} = \mathbf{r}_{\boldsymbol{z}}. \tag{5.8}$$

Let the cyclic permutation $\pi(j) = (j \bmod 2N_{\boldsymbol{z}}) + 1$ for $1 \le j \le 2N_{\boldsymbol{z}}$, which shifts each entry to a smaller index by 1, and the permutation matrix associated with π is $\mathbf{P}_\pi$. Then

$$\mathbf{D}_{\boldsymbol{z}} = \mathbf{I} + \mathbf{P}_\pi = \begin{pmatrix} 1 & 1 & 0 & 0 & \cdots & 0 \\ 0 & 1 & 1 & 0 & \cdots & 0 \\ 0 & 0 & 1 & 1 & \cdots & 0 \\ 0 & 0 & 0 & 1 & \vdots & 0 \\ \vdots & \vdots & \vdots & \vdots & \ddots & \vdots \\ 1 & 0 & 0 & 0 & \cdots & 1 \end{pmatrix}. \tag{5.9}$$

$\mathbf{D}_{\boldsymbol{z},L}$

In order that (5.8) has a solution, $\mathbf{r}_{\boldsymbol{z}}$ is ought to be in the range of $\mathbf{D}_{\boldsymbol{z}}$. When $\mathbf{u}$ is the exact solution (not iterate), the Galerkin orthogonality guarantees this relation holds. Here, the compensation from Section 3 is applied to the approximated residual vector $\mathbf{r}_{\boldsymbol{z}}$. While the interior edge jump entries are kept unchanged, while the element residual entries are modified. Following the procedure presented in Section 3, let $\boldsymbol{\alpha}_{\boldsymbol{z}} \in \mathbb{R}^{2N_{\boldsymbol{z}}}$ be the vector representation of the correction constant (3.15) on $\omega_{\boldsymbol{z}}$:

$$\boldsymbol{\alpha}_{\boldsymbol{z}} = \big(\alpha_{K_1,\boldsymbol{z}}, 0, \alpha_{K_2,\boldsymbol{z}}, 0, \cdots, \alpha_{K_6,\boldsymbol{z}}, 0\big)^T.$$

There is a dimension 1 kernel of $\mathbf{D}_{\boldsymbol{z}}$, which is the scalar multiple of $\nabla^\perp \phi_{\boldsymbol{z}}$. Let $\mathbf{p}_{\boldsymbol{z}} \in \mathbb{R}^{2N_{\boldsymbol{z}}}$ be the vector representation of $\nabla^\perp \phi_{\boldsymbol{z}}$ in the basis (5.6):

$$\mathbf{p}_{\boldsymbol{z}} = \big(-1, 1, -1, 1, \ldots, -1, 1\big)^T \tag{5.10}$$

Then the right hand side of the first equation in (3.12) can be represented by

$$\widetilde{\mathbf{r}}_{\boldsymbol{z}} = \mathbf{r}_{\boldsymbol{z}} - (\mathbf{p}_{\boldsymbol{z}}^T \mathbf{r}_{\boldsymbol{z}}) \boldsymbol{\alpha}_{\boldsymbol{z}}.$$

It can be verified that $\widetilde{\mathbf{r}}_{\boldsymbol{z}}$ is in the range of $\mathbf{D}_{\boldsymbol{z}}$, i.e., it is orthogonal of the kernel vector, $\mathbf{p}_{\boldsymbol{z}}^T\widetilde{\mathbf{r}}_{\boldsymbol{z}} = 0$.

Though $\mathbf{D}_{\boldsymbol{z}}$ is not invertible, but its lower right block $\mathbf{D}_{\boldsymbol{z},L}$, highlighted in (5.9), can be inverted. $\mathbf{D}_{\boldsymbol{z},L}^{-1} \in \mathbb{R}^{(2N_{\boldsymbol{z}}-1)\times(2N_{\boldsymbol{z}}-1)}$ is an upper triangular matrix as follows and can be used to construct the solution vector $\mathbf{s}_{\boldsymbol{z}}$:

$$\mathbf{D}_{\boldsymbol{z},L}^{-1} = \begin{pmatrix} 1 & -1 & 1 & -1 & \cdots & -1 & 1 \\ 0 & 1 & -1 & 1 & \cdots & 1 & -1 \\ 0 & 0 & 1 & -1 & \cdots & -1 & 1 \\ \vdots & \vdots & \vdots & \vdots & \ddots & \vdots & \vdots \\ 0 & 0 & 0 & 0 & \cdots & 0 & 1 \end{pmatrix}.$$

Next step is to assemble the local mass matrix $\mathbf{M}_{\boldsymbol{z}}$ associated with the interior edges on this patch for the discontinuous Raviart-Thomas element space $\boldsymbol{\mathcal{RT}}^0_{-1,\omega_{\boldsymbol{z}}}$. This can be a by-product of Algorithm 3, in that the assembling procedure can be done during the first **for** loop of Algorithm 3. Here the formulas are provided for the integrity. By the local numbering, the first and second interior edges of element K, viewing from the counterclockwise with respect to $\boldsymbol{z}$, are always opposite to the vertices in the 3rd column and the 2nd column of $\mathbf{T}_{\boldsymbol{z}}$, respectively. Let the i ($1 \le i \le N_{\boldsymbol{z}}$) represent the index of K_i, and $\boldsymbol{t}$ be the scaled tangential vector, $\bar{A}$ be the averaging diffusion coefficient on this patch (line 7 in Algorithm 3), and the indices l_j ($j = 1, 2, 3$) follow line 2 in Algorithm 3

$$\boldsymbol{t}_{i,3} = \boldsymbol{z}_{l_2} - \boldsymbol{z}_{l_1},\ \boldsymbol{t}_{i,2} = \boldsymbol{z}_{l_1} - \boldsymbol{z}_{l_3},\ \text{ and }\ \boldsymbol{t}_{i,1} = \boldsymbol{z}_{l_3} - \boldsymbol{z}_{l_2}.$$

Then

$$\begin{aligned} \mathbf{M}_{\boldsymbol{z}}[2i-1, 2i] = \mathbf{M}_{\boldsymbol{z}}[2i, 2i-1] &= -\frac{|\boldsymbol{t}_{i,3}|^2 + |\boldsymbol{t}_{i,2}|^2 + 3\boldsymbol{t}_{i,2}\cdot\boldsymbol{t}_{i,3}}{24\bar{A}|K_i|}, \\ \mathbf{M}_{\boldsymbol{z}}[2i-1, 2i-1] = \frac{|\boldsymbol{t}_{i,3}|^2 - 3\boldsymbol{t}_{i,1}\cdot\boldsymbol{t}_{i,2}}{24\bar{A}|K_i|}, &\quad \mathbf{M}_{\boldsymbol{z}}[2i, 2i] = \frac{|\boldsymbol{t}_{i,2}|^2 - 3\boldsymbol{t}_{i,3}\cdot\boldsymbol{t}_{i,1}}{24\bar{A}|K_i|}, \\ \text{and } \mathbf{M}_{\boldsymbol{z}}[l, m] = 0,\ &\text{if } |l-m| \ge 2. \end{aligned} \tag{5.11}$$

Let the $\mathbf{P}_{\boldsymbol{z}}$ be following matrix having $\mathbf{D}_{\boldsymbol{z},L}^{-1}$ as a block:

$$\mathbf{P}_{\boldsymbol{z}} = \begin{pmatrix} 0 & 0 \\ 0 & \mathbf{D}_{\boldsymbol{z},L}^{-1} \end{pmatrix}.$$

It can be verified that $\mathbf{P}_{\boldsymbol{z}}\widetilde{\mathbf{r}}_{\boldsymbol{z}}$ is a solution of the discrete divergence equation (5.8) (or second and the third equation in (5.1)). Now a minimization procedure (3.16) through projecting the solution orthogonal to the kernel in the weighted L^2-sense is performed:

$$\mathbf{s}_{\boldsymbol{z}} = \mathbf{P}_{\boldsymbol{z}}\widetilde{\mathbf{r}}_{\boldsymbol{z}} - \frac{(\mathbf{P}_{\boldsymbol{z}}\widetilde{\mathbf{r}}_{\boldsymbol{z}})^T\mathbf{M}_{\boldsymbol{z}}\mathbf{p}_{\boldsymbol{z}}}{\mathbf{p}_{\boldsymbol{z}}^T\mathbf{M}_{\boldsymbol{z}}\mathbf{p}_{\boldsymbol{z}}}. \tag{5.12}$$

Lastly, the local total error indicator and the global error estimate is computed by:

$$\eta_{D,\,\boldsymbol{z}} = \left(\mathbf{s}_{\boldsymbol{z}}^T\mathbf{M}_{\boldsymbol{z}}\mathbf{s}_{\boldsymbol{z}}\right)^{1/2},\ \text{ and }\ \eta_D^2 = \sum_{\boldsymbol{z}\in\mathcal{N}} \frac{1}{N_{\boldsymbol{z}}}\eta_{D,\,\boldsymbol{z}}^2. \tag{5.13}$$

6 Numerical examples

In this this section, several examples are presented to verify the reliability and effectivity of the estimators proposed, as well as the stopping criterion. The localized equilibrated flux type error estimator is implemented in *i*FEM ([18]). The initial guess for all examples presented in this section is a random guess with each entry of $\mathbf{u}^{(0)}$ satisfying a uniform distribution in $[-1, 1]$ using a fixed seed. Knowing that, in practice, when the solution $u_{\mathcal{T}}$ from direct solve is used, the effectivity index $\varepsilon \approx 1.5$ for η_D in the pre-asymptotic regime, where ε is defined by $\varepsilon := \eta_D / \left\|u - u_{\mathcal{T}}\right\|_A$. Using the identity (1.2), empirically, the discretization contribution to the total error is approximately $\eta_D/1.5$. Now by Theorem 4.4, to balance the contribution of the algebraic error and discretization error, it is reasonable to set the tolerance $\texttt{tol} = 2/3 \approx 0.67$ in Algorithm 1.

Example 1: the true solution for both example 1 and 2 is: for $(x, y) \in (-1, 1)^2$

$$u = a\Big(\sin(\pi x)\sin(\pi y) + 0.5\sin(4\pi x)\sin(4\pi y)\Big).$$

The constant a is chosen such that $\|u\|_A = 1$. u solves $-\Delta u = f$ with diffusion coefficient $A = 1$. The problem is discretized on a uniform triangular mesh with $h = 1/32$. The solver for is using an unpreconditioned multigrid $V(1, 1)$-cycle. The convergence result for the solver is in Figure 2a. The estimated $\rho^{(k)}$ in Figure 2b is presented to verify Theorem 4.4. Moreover, Theorem 4.4 is verified in Figure 2a for η_A being an upper bound of the algebraic error. In this example, for testing purpose, only $\eta_A \leq (\texttt{tol})\eta_D$ from Algorithm 1 is used as stopping criterion, for there is only 1 level and no AFEM cycles are performed. This stopping criterion is satisfied at iteration number 2. Meanwhile, it is observed that the algebraic error $\left\|u_h - u_h^{(k)}\right\|_A$ drops below the total error $\left\|u - u_h^{(k)}\right\|_A$ after the 2nd iteration ($k = 2$, see Figure 2a).

For illustration purpose, the solver is allowed to run more iterations. The comparison of direct-solved u_h and the multigrid iteration at the 2nd iteration is shown in Figure 3. The local efficiency of the total error estimator $\eta_{D,K}$ is shown in Figure 4. For this example, if conventional way of using relative residual measured in ℓ^2-norm $\left\|\mathbf{A}\mathbf{e}^{(k)}\right\|_0 / \left\|\mathbf{A}\mathbf{e}^{(0)}\right\|_0$ as a stopping criterion is practiced, choosing a tolerance being 10^{-7} results the $V(1, 1)$-cycle iterations stop at iteration number 15. We compare the different components in total error $\left\|u - u_h^{(k)}\right\|_A$ when the solver stops according to different stopping criteria in Table 1.

Example 2: this example uses the same problem and dicretization with Example 1. In this example, we choose to test the stopping criteria for an unpreconditioned symmetric Gauss-Seidel sweeping. It is known that GS has a much slower rate of convergence than multigrid. Other than the stopping criterion in Algorithm 1, we compare another stopping criterion: if the relative residual $\|\mathbf{r}_k\|_2 / \|\mathbf{r}_0\|_2 \leq 10^{-5}$, the solver stops. The comparison with the stopping criterion in Algorithm 1 is compiled in Table 1.

Table 1: Comparison of error contributions when the iterative solver stops using different stopping criteria, the disretization error in all cases is $\|u - u_{\mathcal{T}}\|_A \approx 0.0741$. The second column stands for the iteration number when the stopping criteria are met and the solver stops.

	Stopping	# Iter	$\|u - u_{\mathcal{T}}^{(k)}\|_A$	$\|u_{\mathcal{T}} - u_{\mathcal{T}}^{(k)}\|_A$
Example 1	$\eta_A \leq 0.67\eta_D$	2	0.0821	0.0352
Example 1	$\frac{\|\mathbf{r}_k\|_2}{\|\mathbf{r}_0\|_2} \leq 10^{-7}$	15	0.0741	$3.4272 \cdot 10^{-8}$
Example 2	$\eta_A \leq 0.67\eta_D$	31	0.1051	0.0745
Example 2	$\frac{\|\mathbf{r}_k\|_2}{\|\mathbf{r}_0\|_2} \leq 10^{-5}$	289	0.0741	$2.7144 \cdot 10^{-4}$

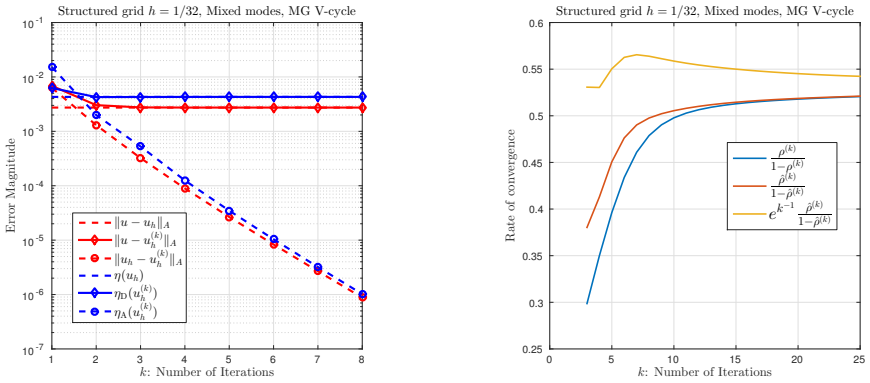

(a) The convergence of the $V(1,1)$-cycles. (b) The convergence of the estimated rate of convergence

Figure 2: The convergence results for Example 1: the solution has mixed modes, the problem is dicretized on a uniform triangular mesh, and the linear system is approximated using $V(1,1)$-cycle iterations.

Example 3: this example tests the inexact AFEM cycles in Algorithm 1 for the Kellogg intersecting interface problem. The Kellogg problem with a checkerboard coefficient distribution, constructed back in [12], is commonly used benchmark for testing the efficiency and robustness of the a posteriori error estimator ([16, 13, 14, 20, 31]):

$$-\nabla\cdot(A\nabla u) = 0, \text{ in } \Omega = (-1,1)^2. \tag{6.1}$$

$$A = \begin{cases} R & \text{in } (0,1)^2 \cup (1,0)^2, \\ 1 & \text{in } \Omega\backslash\Big((0,1)^2 \cup (1,0)^2\Big). \end{cases}$$

The exact solution u of (3.2) is given in polar coordinates (r,θ):

$$u = r^{\gamma}\psi(\theta) \in H^{1+\gamma-\epsilon}(\Omega) \quad \text{for any} \quad \epsilon > 0,$$

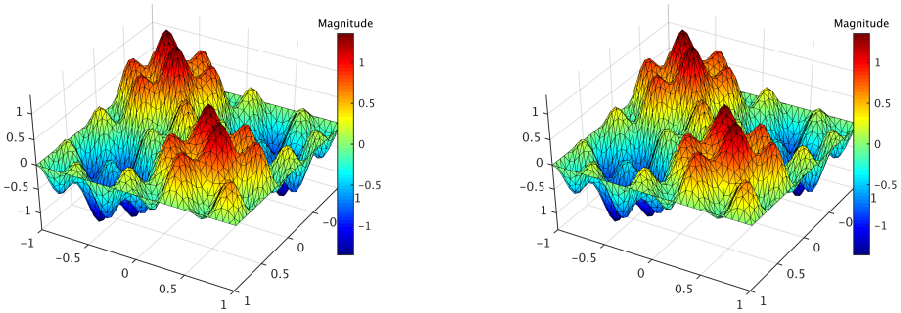

(a) u_h obtained by a direction solver.

(b) $u_h^{(2)}$ obtained by $V(1,1)$-cycles.

Figure 3: The comparison of the direct-solved approximation u_h and the multigrid iterate $u_h^{(2)}$ in Example 1.

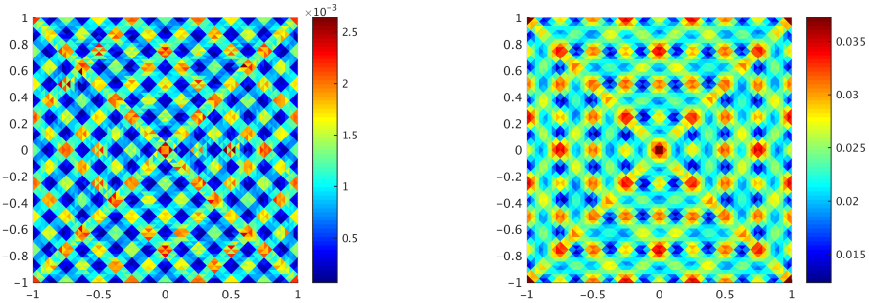

(a) Local energy error $\left\|u - u_h^{(2)}\right\|_{A,K}$.

(b) Local total error indicator $\eta_{D,K}$ in (3.21).

Figure 4: The comparison of the total local error and the local error estimator in Example 1.

where for the definition of $\psi(\theta)$ please refer to [20]. Here we set the parameter to be:

$$\gamma = 0.5, \quad R \approx 5.8284271247461907, \quad \rho = \pi/4, \text{ and } \sigma \approx 2.3561944901923448.$$

The AFEM cycles is applied to this problem. If the step "ITERATE" is replace with a direct solve, Algorithm 1 becomes an exact AFEM cycle. On a triangulation $\mathcal{T}_m$, we use exact AFEM cycle when $\#(\mathtt{DoF}_m) \geq 500$. For the step "MARK", we opt Dörfler marking strategy and mark the elements in the bulk with the largest error indicators which contributes to the 50% of the total error estimator in L^2-sense. For the step "REFINE", bisection is used.

Provided the meshes are adaptively refined during the AFEM cycles, to determine whether the discretized system problems need to be approximated to the machine precision as in a direct solve (exact), or certain iterations of an MG V-cycles suffice (inexact), a key measure is to check the rates of convergence r,. The rate of convergence

r (notice this is different from the rate of convergence ρ_{err} for the solver in Section 4) satisfies the following:

$$\left\|u - \bar{u}_{\mathcal{T}_m}\right\|_A \sim O(\#(\texttt{DoF}_m)^{-r}), \tag{6.2}$$

where m stands for the numbering of the different levels of triangulations $\{\mathcal{T}_m\}$, and $\#\texttt{DoF}_m$ is the number of degrees of freedom on $\mathcal{T}_m$. $\bar{u}_{\mathcal{T}_m}$ is the final output of the iterative solver on $\mathcal{T}_m$ when exiting. Note that, if the iterate $\bar{u}_{\mathcal{T}_m}$ is replaced by the direct solve approximation $u_{\mathcal{T}_m}$, and the mesh has been adaptively refined with an efficient local indicator to produce a sequence of meshes $\mathcal{T}_1 \subset \mathcal{T}_2 \subset \cdots \subset \mathcal{T}_m$, the optimal rate of convergence is $O(\#(\texttt{DoF}_m)^{-1/2})$ predicted by the a posteriori error estimator's reliability bound for the direct solve $u_{\mathcal{T}_m}$. This is to say, the optimal rate is achieved with $r \approx 1/2$. Now if r is close to $1/2$ for an inexact AFEM cycle, this in turn implies that the stopping criterion produces an accurate enough approximation to properly guide the adaptive mesh refining procedure.

Another measure is the effectivity index ε for the total error estimator on the finest level of mesh:

$$\varepsilon := \frac{\eta_D(\bar{u}_{\mathcal{T}_m})}{\left\|u - \bar{u}_{\mathcal{T}_m}\right\|_A}. \tag{6.3}$$

For this example, we choose $\texttt{tol} = 0.67$ and $\texttt{tol}_\rho = 0.1$ for the stopping criterion in Algorithm 1. The $k = 3$ in Algorithm 1, which means the stopping criterion is checked every three $V(1,1)$-cycles. Both the rate of convergence and the effectivity index are reported in Table 2. Table 2 also contains the number of AFEM cycles needed to reach a relative error of $\left\|u - \bar{u}_{\mathcal{T}_m}\right\|_A / \|u\|_A < 1\%$, starting from the mesh with $\#(\texttt{DoF}) = 320$. The adaptively generated meshes for both exact and inexact AFEM cycle with $\#(\texttt{DoF}) \approx 2000$ are shown in Figure 6. The local error distribution is shown in Figure 7.

Table 2: Comparison of the convergence of the inexact AFEM cycle Algorithm 1 to the AFEM cycle with exact solve in Example 3 when the relative error is approximately 1%. r is the rate of convergence, ε is the effectivity index, and $m = \#$(AFEM cycles) performed. The ($\#\texttt{Dof}$) and relative energy error are the ones on the finest level.

	r	ε	m	# Dof	$\left\|\text{error}_{\mathcal{T}_m}\right\|_A / \|u\|_A$
Inexact AFEM	0.53996	1.4542	14	20337	0.008857
Exact AFEM	0.55085	1.4495	14	20359	0.008829

References

[1] M. Arioli, E. H. Georgoulis, and D. Loghin, *Stopping criteria for adaptive finite element solvers*, SIAM Journal on Scientific Computing, 35 (2013), pp. A1537–A1559. 2

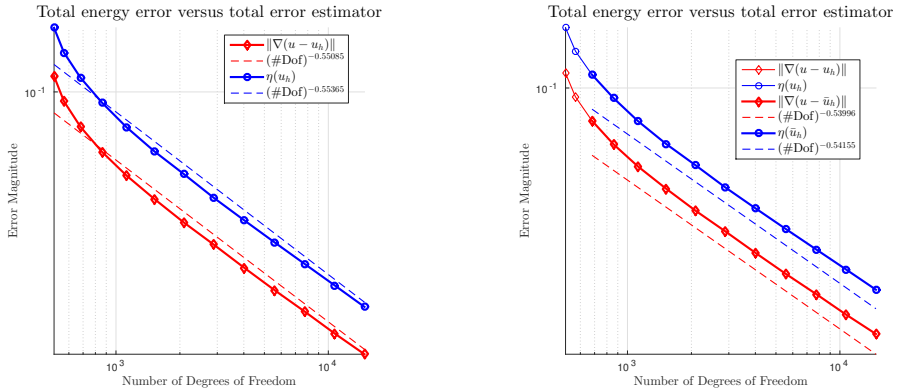

(a) The convergence of the exact AFEM cycles.

(b) The convergence of the inexact AFEM cycles.

Figure 5: The convergence results of the inexact vs exact AFEM cycles for Example 3: when the $\#(\mathtt{DoF}_m) \geq 500$, the iterative solver is adopted for the discretized liner system.

[2] M. Arioli, J. Liesen, A. Miedlar, and Z. Strakoš, *Interplay between discretization and algebraic computation in adaptive numerical solution of elliptic PDE problems*, STFC, 2012. 2

[3] M. Arioli, D. Loghin, and A. J. Wathen, *Stopping criteria for iterations in finite element methods*, Numerische Mathematik, 99 (2005), pp. 381–410. 2

[4] R. E. Bank and R. K. Smith, *A posteriori error estimates based on hierarchical bases*, SIAM Journal on Numerical Analysis, 30 (1993), pp. 921–935. 2

[5] R. E. Bank and J. Xu, *Asymptotically exact a posteriori error estimators, part i: Grids with superconvergence*, SIAM Journal on Numerical Analysis, 41 (2003), pp. 2294–2312. 2

[6] R. Becker, C. Johnson, and R. Rannacher, *Adaptive error control for multigrid finite element*, Computing, 55 (1995), pp. 271–288. 2

[7] C. Bernardi and R. Verfürth, *Adaptive finite element methods for elliptic equations with non-smooth coefficient*, Numerische Mathematik, 85 (2000), pp. 579–608. 10

[8] D. Braess, *Finite Elements: Theory, Fast Solvers, and Applications in Solid Mechanics*, Cambridge University Press, 2007. 8

[9] D. Braess and J. Schöberl, *Equilibrated residual error estimator for edge elements*, Math. Comp., 77 (2008), pp. 651–672. 3, 8, 13

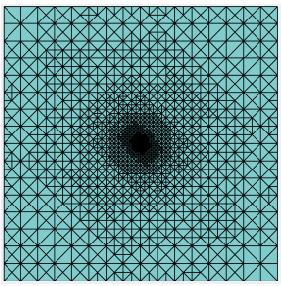

(a) Adaptively refined mesh using the exact AFEM cycle.

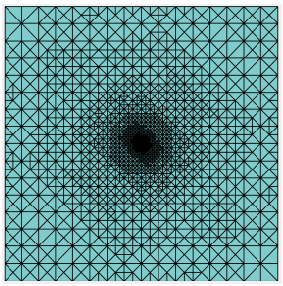

(b) Adaptively refined mesh using the inexact AFEM cycle Algorithm 1.

Figure 6: The comparison of adaptive mesh generation for exact and inexact AFEM cycles.

[10] F. Brezzi and M. Fortin, *Mixed and Hybrid Finite Element Methods*, Springer, 1991. 9

[11] W. L. Briggs, V. E. Henson, and S. F. McCormick, *A multigrid tutorial*, Siam, 2000. 5

[12] R. Bruce Kellogg, *On the poisson equation with intersecting interfaces*, Applicable Analysis, 4 (1974), pp. 101–129. 28

[13] Z. Cai and S. Cao, *A recovery-based a posteriori error estimator for h(curl) interface problems*, Computer Methods in Applied Mechanics and Engineering, 296 (2015), pp. 169–195. 28

[14] Z. Cai, S. Cao, and R. Falgout, *Robust a posteriori error estimation for finite element approximation to h(curl) problem*, Computer Methods in Applied Mechanics and Engineering, 309 (2016), pp. 182–201. 28

[15] Z. Cai, X. Ye, and S. Zhang, *Discontinuous galerkin finite element methods for interface problems: a priori and a posteriori error estimations*, SIAM Journal on Numerical Analysis, 49 (2011), pp. 1761–1787. 10

[16] Z. Cai and S. Zhang, *Robust equilibrated residual error estimator for diffusion problems: Conforming elements*, SIAM J. Numer. Anal., 50 (2012), pp. 151–170. 3, 8, 13, 20, 24, 28

[17] Z. Cai and S. Zhang, *Finite element methods for interface problems: Robust and local optimal a priori error estimates*, arXiv preprint arXiv:1509.08166, (2015). 11

[18] L. Chen, *iFEM: an innovative finite element methods package in MATLAB*, (2008). 21, 27

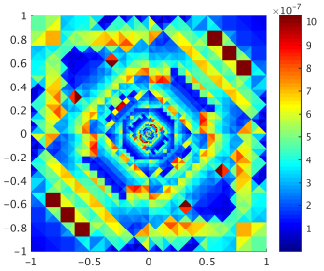

(a) Local error $\|u - u_{\mathcal{T}}\|_{A,K}$.

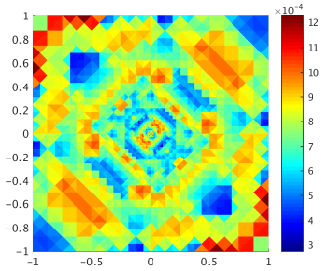

(b) Local error indicator $\eta_{D,K}$ in (3.21) using direct solve $u_{\mathcal{T}}$.

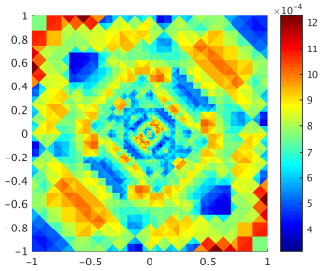

(c) Local error indicator $\eta_{D,K}$ using iterate $\bar{u}_{\mathcal{T}}$.

Figure 7: The comparison the local error and error indicator distribution for exact and inexact AFEM cycles.

[19] L. Chen, M. Holst, and J. Xu, *Convergence and optimality of adaptive mixed finite element methods*, Mathematics of Computation, 78 (2009), pp. 35–53. 9

[20] Z. Chen and S. Dai, *On the efficiency of adaptive finite element methods for elliptic problems with discontinuous coefficients*, SIAM Journal on Scientific Computing, 24 (2002), pp. 443–462. 28, 29

[21] P. Destuynder and B. Métivet, *Explicit error bounds in a conforming finite element method*, Mathematics of Computation of the American Mathematical Society, 68 (1999), pp. 1379–1396. 3

[22] V. Dolejší, I. Šebestová, and M. Vohralík, *Algebraic and discretization error estimation by equilibrated fluxes for discontinuous galerkin methods on non-matching grids*, Journal of Scientific Computing, (2013), pp. 1–34. 2, 3

[23] W. Dörfler and R. H. Nochetto, *Small data oscillation implies the saturation assumption*, Numerische Mathematik, 91 (2002), pp. 1–12. 2

[24] M. Dryja, M. V. Sarkis, and O. B. Widlund, *Multilevel schwarz method for elliptic problems with discontinuous coefcients in three dimensions*, Numerische Mathematik, 72 (1996), pp. 313–348. 10

[25] I. Ekeland and R. Temam, *Convex analysis and variational problems*, (1976). 3, 7

[26] R. D. Falgout and U. M. Yang, hypre*: A library of high performance preconditioners*, in International Conference on Computational Science, Springer, 2002, pp. 632–641. 20

[27] P. Jiránek, Z. Strakoš, and M. Vohralík, *A posteriori error estimates including algebraic error and stopping criteria for iterative solvers*, SIAM Journal on Scientific Computing, 32 (2010), pp. 1567–1590. 2, 3

[28] T. V. Kolev and P. S. Vassilevski, *Parallel auxiliary space amg for h(curl) problems*, Journal of Computational Mathematics, (2009), pp. 604–623. 20

[29] R. Luce and B. I. Wohlmuth, *A local a posteriori error estimator based on equilibrated fluxes*, SIAM Journal on Numerical Analysis, 42 (2004), pp. 1394–1414. 3

[30] D. Meidner, R. Rannacher, and J. Vihharev, *Goal-oriented error control of the iterative solution of finite element equations*, Journal of numerical mathematics, 17 (2009), pp. 143–172. 2

[31] M. Petzoldt, *A posteriori error estimators for elliptic equations with discontinuous coefficients*, Advances in Computational Mathematics, 16 (2002), pp. 47–75. 10, 28

[32] R. Rannacher, *Error control in finite element computations*, Springer, 1999. 2

[33] R. Verfürth, *A review of a posteriori error estimation and adaptive mesh-refinement techniques*, vol. 1, Wiley-Teubner Chichester, 1996. 14

[34] R. Verfürth, *A note on constant-free a posteriori error estimates*, SIAM Journal on Numerical Analysis, 47 (2009), pp. 3180–3194. 3

[35] J. Xu and Z. Zhang, *Analysis of recovery type a posteriori error estimators for mildly structured grids*, Mathematics of Computation, 73 (2004), pp. 1139–1152. 2